An Electronically Addressed Spatial Light Modulator

Douglas J. McKnight

Submitted for the degree of
PhD

Department of Physics
University of Edinburgh
1989

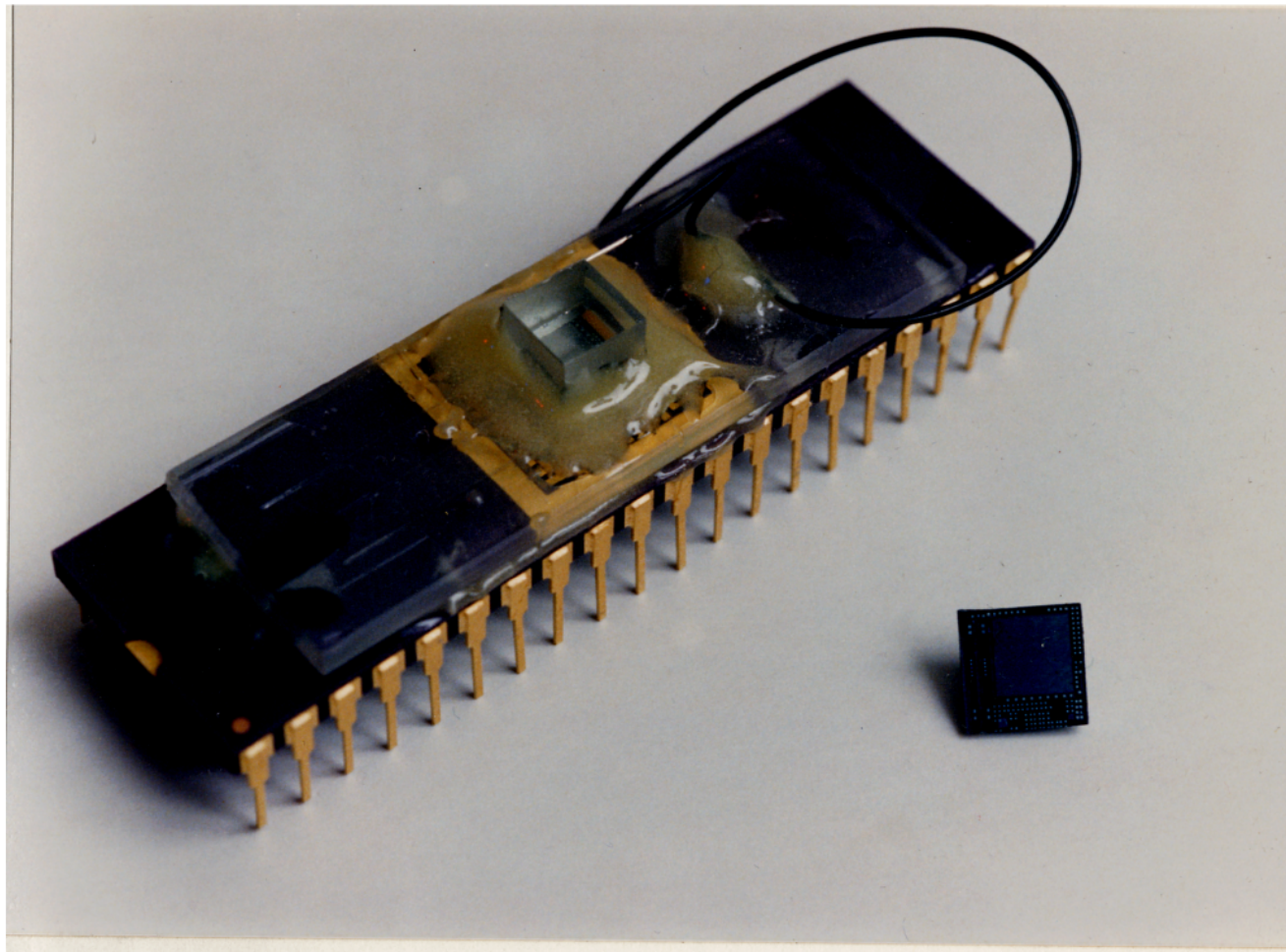

Frontispiece: A 50 × 50 spatial light modulator with, beside it, the integrated circuit which controls the liquid crystal light modulating layer. The integrated circuit can be seen inside the complete device through the cover glass.

Acknowledgements

It would not be possible to thank properly everyone who has helped me during the course of this work. My special thanks go to my supervisors, David Vass and Dick Sillitto, who have always been readily available to discuss the project. Most other members of the Applied Optics group also deserve thanks for their contribution. In particular I would like to thank Ian Underwood who designed the prototype IC, the use of which is described in chapter 2 Mike Ranshaw who has helped with the proofreading and Andy Garrie for technical assistance. Zhaojian Chen of the EMF was responsible for the wafer processing and it is through his care that the devices worked. Rod Widdowson helped with access to IC data processing software. Further, the friends I have made over the years have contributed to my education as well as to my enjoyment of my time in Edinburgh. They have been an essential part of it all. My mother deserves thanks both for her continued tolerance and for her enthusiastic participation in the Hogmanay celebrations of 1962. It is to her that I dedicate this thesis.

Declaration

I declare that the composition of this thesis, and all the work described within it, was carried out by me, except where otherwise acknowledged.

Douglas M'Knight

Abstract

Coherent optical data processing is recognised to be a natural solution to certain information processing problems. Attempts to exploit the benifits of optical processing are limited by the quality of available Spatial Light Modulators. Spatial Light Modulators are devices which controllably impress information onto the amplitude or phase of an optical wavefront. They are used both to input data into an optical system and as modulating elements within the system (often in the Fourier plane of a Fourier transform processor).

This thesis describes the successful development of an electronically addressed spatial light modulator using liquid crystal as the light modulating material and a silicon integrated circuit as the addressing medium. It is a pixelated binary spatial light modulator operating in reflection. Each pixel contains a memory element which stores the programmed logical state of the pixel. The addressing and pixel circuits were fabricated in a 1.5μm nMOS technology on a 10 mm square chip. The pixels are arranged on a square array containing 50×50 elements. The liquid crystal was configured to modulate the light amplitude using the hybrid field effect in a nematic liquid crystal.

The spatial light modulator is used as a Fourier plane filter in a coherent optical processing system. Its performance is assessed and the direction of future research into this type of spatial light modulator is discussed.

Glossary

ADC	Analogue to Digital Converter.
CCD	Charge Coupled Device.
CMOS	Complementary Metal-Oxide-Silicon.
die	The area of the silicon wafer which will become a chip when the wafer is sawn up.
E7	A nematic liquid crystal mixture.
EMF	Edinburgh Microfabrication Facility.
Fill factor	The fraction of the total pixel area which is optically useful (mirror).
FLC	Ferro-electric Liquid Crystal.
FT	Fourier Transform.
HFE	Hybrid Field Effect (in liquid crystals).
IC	Integrated Circuit.
ITO	Indium Tin Oxide.
LCLV	Liquid Crystal Light Valve.
LED	Light Emitting Diode.
NDA	Negative Dielectric Anisotropy.
nMOS	n-channel Metal-Oxide-Silicon.
PDA	Positive Dielectric Anisotropy.
pMOS	p-channel Metal-Oxide-Silicon.
PSF	Point spread function (of an optical imaging system).
PVA	Poly Vinyl Alcohol.
SLM	Spatial Light Modulator.
TFT	Thin Film Transistor.
TN	Twisted Nematic.
VCB	Voltage-controlled birefringence.
VLSI	Very Large Scale Integration.

Contents

Chapter 1

Introduction: Spatial Light Modulators and Optical Data Processing

A Spatial Light Modulator (SLM) is a device which can impress information onto an optical wavefront. Such devices range from the simple photographic transparency to the various types of electronically and optically controlled spatial light modulators which are the subject of much current research.

In this section SLMs will be described in a general way as an introduction to a discussion of some specific devices. There follows a discussion of some applications of SLMs including the area of Fourier optical information processing which is addressed later in this thesis.

The final section in this chapter outlines the structure of the rest of the thesis and relates this to the aims of the project.

1.1 Spatial light modulation

In general, the function of a spatial light modulator is to multiply a two dimensional optical data field (an image) by a two dimensional modulation function. In the case of a photographic transparency the modulation function, or trans-

mission in this case, is fixed when the film is exposed and processed. To realise the full potential of systems which exploit this simultaneous point-by-point multiplication, SLMs which can be reconfigured in "real time" are required.

Devices exist which can perform this function. They can be placed in various categories depending on

1. the way the modulation information is sent to the SLM — *addressing*
2. the way the device interacts with the incoming light — *modulation.*

1.1.1 Addressing schemes

Spatial light modulators can be addressed optically or electronically.

Optically addressed SLMs

The modulation function of an optically addressed SLM is configured by projecting a "write" image onto its light sensitive address surface, see figure 1.1. The modulation of the "read" image depends on the intensity of the write image — the form of the relationship varies widely from device to device.

Electronically addressed SLMs

Electronically addressed SLMs modulate an incident image as a function of an electronically loaded data set. They are usually pixelated devices and often can operate in transmission, unlike conventional optically addressed devices. They are used as the interface between electronic and optical data processing systems.

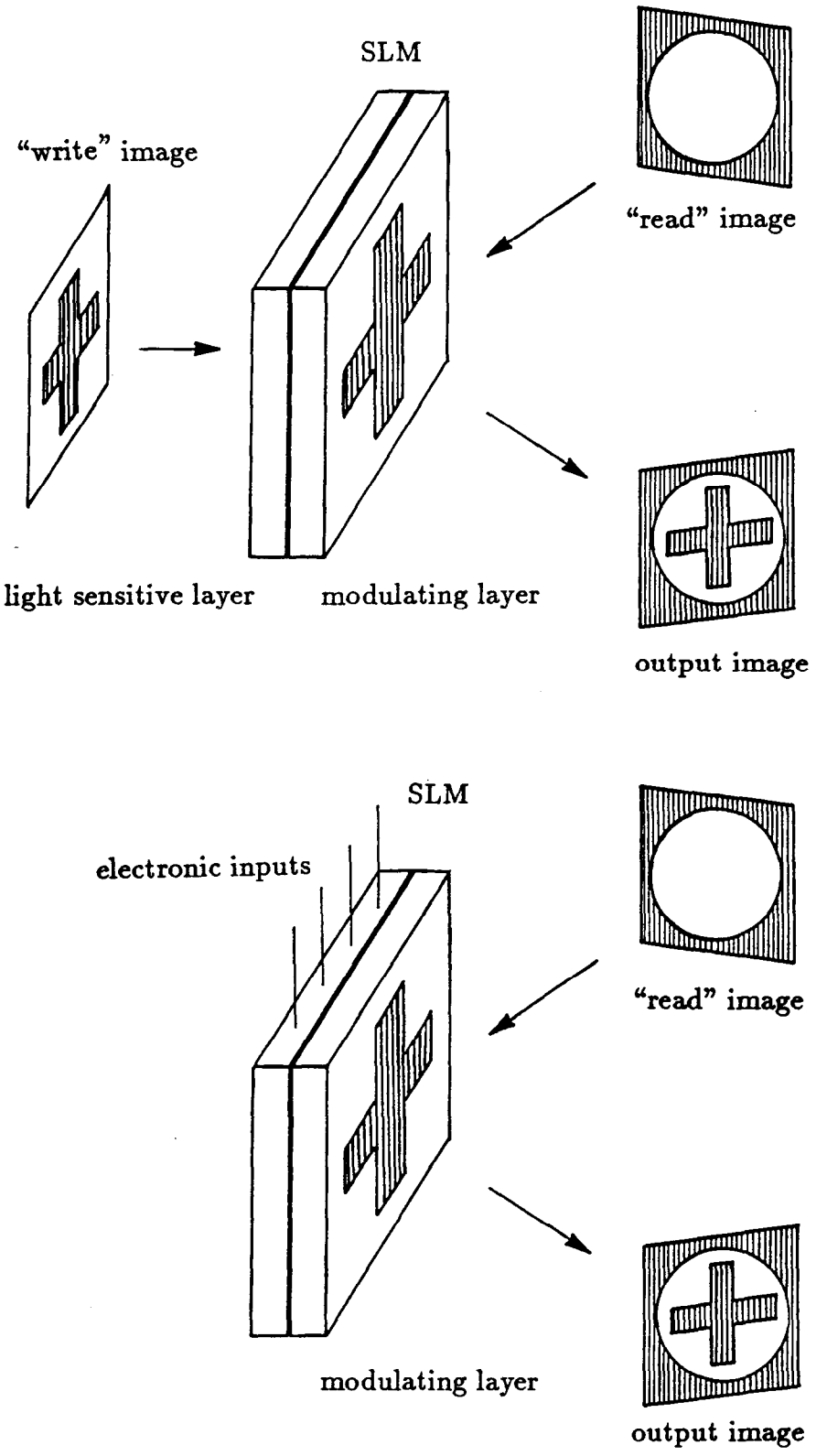

Figure 1.1: Optical and electronic addressing of spatial light modulators. The basic operation of an SLM, which is to multiply an input (or "read") image by a modulation function, is illustrated here.

1.1.2 Light modulation

The input light field can be modulated in intensity,

$$I_{output}(x,y) = m(x,y).I_{input}(x,y) \tag{1.1}$$

or, in coherent illumination the complex-amplitude, $\tilde{u}$, can be modulated

$$\tilde{u}_{output}(x,y) = \tilde{m}(x,y).\tilde{u}_{input}(x,y) \tag{1.2}$$

where $\tilde{u} = ue^{i\phi(x,y)}$ and $\tilde{m} = me^{i\psi(x,y)}$. An ideal complex-amplitude modulating SLM would allow control of the amplitude and the phase of the signal at each point of the data field. Most of the research in SLM construction is directed towards pure amplitude or pure phase modulation. Full complex-amplitude modulation could be realised by cascading suitable phase and amplitude modulators in the same system.

The modulation in phase, amplitude or intensity can be continuous or discrete. Devices which offer discrete levels of modulation are usually electronically addressed binary devices. That is, they have two modulation states. In amplitude modulators these are usually "on" and "off"; $m(x,y)$ takes a value as close to 1 or 0 as possible.

1.1.3 Spatial light modulator performance issues

There are many factors involved in the assessment of a particular SLM, and their relative importance depends on the application. A feature which is a disadvantage in one application may be an advantage in others. An example of this is a non-linear response in an optically addressed SLM which, although useful for some applications like for example thresholding in an optical neural network, makes direct incoherent to coherent conversion of a continuous grey scale image impossible.

Another problem with device assessment is that often performance parameters are coupled. In these cases the performance measurements depend on the particular trade-off chosen when the measurements are made. For example, in many devices, spatial resolution and modulation depth are linked so the device specification can only really be made with reference to the modulation transfer function (MTF).

In general the performance factors can be roughly grouped as follows.

	Unpixelated	Pixelated
Modulation	Resolution, aperture, MTF, uniformity, optical flatness, switching speed.	Number of pixels, fill factor,[1] binary/grey scale, contrast ratio, uniformity, optical flatness, switching speed.
	Optical	**Electronic**
Addressing	(Spectral) sensitivity, optical resolution, addressing speed.	Complexity of peripherals, addressing speed.
General	Storage capability, image processing features, complexity, lifetime.	

1.2 A review of current spatial light modulators

Many different light modulation and addressing techniques have been combined to make SLMs. A complete review of SLM technology is found in the papers by Fisher and Lee [21], and Casasent [11]. Recent reports of the development of

[1]The fraction of the total pixel area that is optically useful.

most types of SLM are found in the conference proceedings of the Optical Society of America Topical Meeting on Spatial Light Modulators and Applications [2]. In this section devices which are widely used, interesting or directly relevant to this project are reviewed.

1.2.1 Optically addressed liquid crystal spatial light modulators

Many of the optically addressed devices have a structure similar to the Hughes Liquid Crystal Light Valve (LCLV) [28]. The device is illustrated in figure 1.2. It uses Cadmium Sulphide (CdS) as a photoconductor to control the fraction of an ac drive signal which is dropped across the liquid crystal light modulating layer. Liquid crystal materials are commonly used as the modulating material in SLMs because of their large optical response to low drive voltages. The Hughes LCLV uses the Hybrid Field Effect (HFE) which is described in section 2.1.2.

The CdS layer suffers from a slow response time and Efron et al. working at Hughes, developed a silicon addressed version of the device [18]. The CdS is replaced by a silicon photodetector. Implanted microdiodes gather the photogenerated charge and prevent image smearing. Similar devices have been developed by GEC [37], and by Lockheed [5]. The Lockheed device uses gallium arsenide as the photoconductor and relies on surface traps to restrict charge smearing. This device has been used in an edge enhancing or image differentiating mode, an example of a useful image processing function performed on the SLM [4,6]. A spatial light modulator using a BSO photo-conductor has been developed by British Aerospace [7].

1.2.2 Electrically addressed liquid crystal SLMs

Virtually all the electrically addressed liquid crystal SLMs are pixelated. An interesting exception is the e-beam addressed device developed by Optron systems [30]. A proprietary electron gun (as used in high resolution monitors) is used to

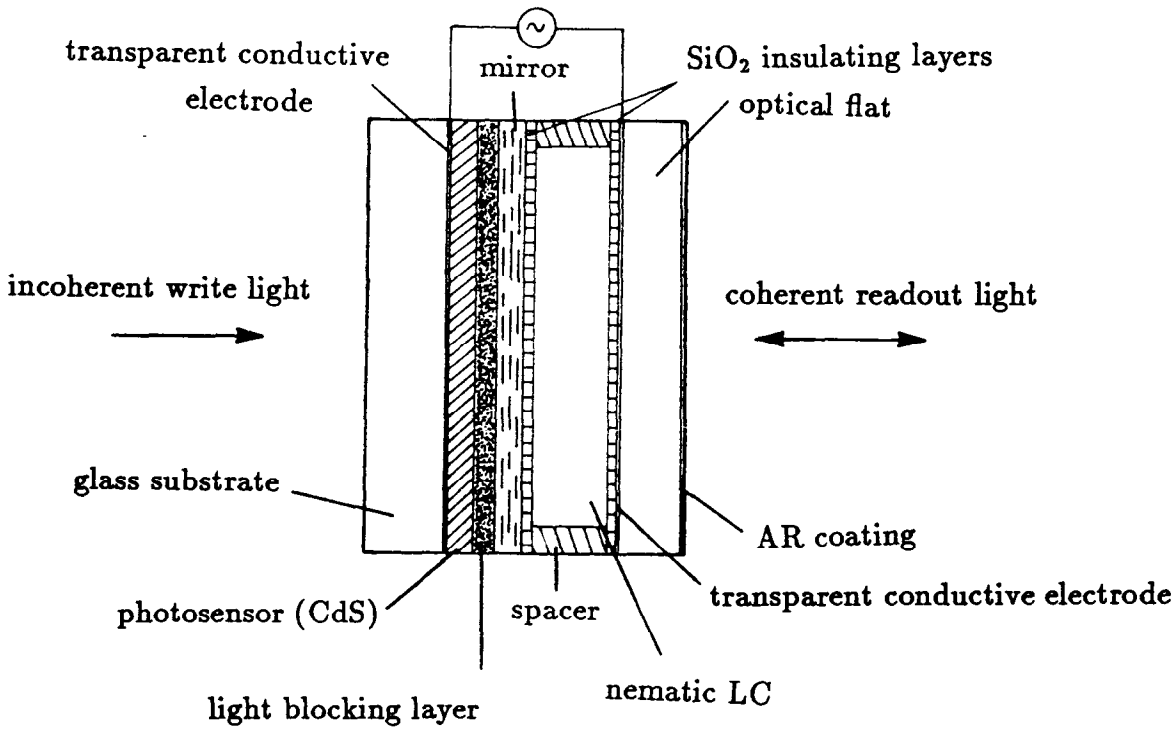

Figure 1.2: The structure of the Hughes optically addressed LCLV

write charge to a "charge transfer plate". This consists of a densely packed array of small conducting pins embedded in an insulating substrate. It is polished flat to form one of the walls of a conventional liquid crystal cell. The structure of the device requires a reflective readout as used in conventional optically addressed devices.

Ferroelectric liquid crystal multiplexed arrays

The simplest way to address a matrix of pixels is to use multiplexed row and column addressing. Each pixel is formed by the intersection of a transparent row electrode on one side of the LC layer and a transparent column electrode on the other. Data is simultaneously presented to all the columns, and one row at a time is selected by an appropriate voltage signal. There is an error voltage present which affects the unselected rows. The effect the error voltage has depends on the size of array being addressed and the characteristics of the liquid crystal used. Needham [45] discusses the limitations of multiplexed addressing in its application to twisted nematic displays. The recent development of Ferroelectric liquid crystals (FLCs) has improved the performance obtainable with this type of addressing. FLCs allow construction of large arrays because the inherent bistability of the FLC is sufficiently strong that the state of the pixel (in the logical sense) is not affected by the error voltages. At present the best multiplexed FLC SLMs are built by STC Technology [9,14]. A 64×64 pixel device and recently a 128×128 pixel device have been demonstrated [54]. This approach does have some disadvantages. Although the *state* of the pixel is not changed by the error voltages, the liquid crystal is disturbed enough to reduce the pixel contrast significantly. In the 64×64 STC device the contrast ratio[2] of a pixel addressed as part of the array is 35:1 which compares poorly with $> 1000 : 1$ for a directly addressed pixel. In this scheme the addressing speed is limited by the liquid crystal response time. The signal has to be present on each column long enough to change the state of the liquid crystal at the pixels.

[2]Defined as the intensity transmitted by an "on" pixel : the intensity transmitted by an "off" pixel, in uniform illumination.

Even fast FLCs are quite slow compared with electronic addressing speeds.

Active matrix SLMs

The active matrix approach addresses these problems by incorporating a transistor at each pixel. The array is scanned electronically with the pixel transistor performing a sample and hold function. The data is sampled when the transistor is "on", and held by the pixel capacitance until the next refresh. The time taken to address the array can be reduced because there is no need to wait for each column of pixels to reset before moving to the next one, the contrast can also be expected to improve because there is no error voltage present.

This design has been implemented in Thin Film Transistors (TFTs) for use in displays. Some recent displays are of a high enough quality that research into their use in optical processing applications is being carried out [69,41]. The problems with these devices tend to be poor optical flatness and low contrast [39]. Also the electrical characteristics of TFTs are not as good as those of silicon transistors. Present collaborative work between the University of Edinburgh Physics Department and STC Technology is directed towards fast single transistor SLMs using ferroelectric liquid crystals. The transistors are to be implemented in single crystal silicon as part of an integrated circuit. Array sizes of 256^2 and 512^2 pixels are planned.

Greater complexity at each pixel

It is possible to exploit integrated electronics by building more complexity into the SLM structure. This has been done in one way by Efron et al. [17], who have used a CCD array as the input to a silicon LCLV. Analogue shift registers are used to establish a "charge image" on the CCD array. This is then released into the silicon layer where it fulfils the same function as the photo-induced charge in the optically addressed device.

Underwood, working at the University of Edinburgh, has used standard integrated circuit (IC) technology to construct an SLM with built-in electronic memory [61,62]. This work is the direct forerunner of the work in this thesis and, as such, will be described in some detail. The device is a pixelated binary amplitude modulator which uses a guest-host liquid crystal as the light modulating layer (see section 2.1.2) and an nMOS IC as the address mechanism. The pixels have a centre to centre spacing of 200μm on a square array of 16 $\times$ 16 elements. Each pixel contains a 100μm$\times$100μm reflective mirror/electrode surrounded by circuitry. The circuitry at each pixel stores one bit of data, which specifies the state of the pixel, and generates a suitable ac signal to drive the LC layer. The on-pixel memory is static; once an image is loaded it does not have to be refreshed. The array of memory elements is addressed by row DATA wires and column ENABLE wires, a total of 32 inputs to the IC. These inputs can be controlled by a microcomputer or driven directly by switches. The IC will function over a range of voltages and this flexibility has allowed it to be used in a number of SLM experiments at the University of Edinburgh. Its use as a test bed for a liquid crystal configuration is described later in this thesis, see section 2.2.3. It has also been used by Ranshaw [50] to address pure phase modulators using liquid crystal and deformable membrane modulation layers.

1.2.3 Other spatial light modulator technologies

Magneto-optic devices

Electrically addressed SLMs have been constructed using the Faraday effect to rotate the plane of polarisation of light transmitted through a film of magneto-optic material. The film is formed into isolated domains or pixels, each of which can be switched between two stable states. These states rotate the polarisation plane of incident light in opposite directions. Suitably oriented polarisers allow either binary amplitude modulation or binary phase modulation. Thermally induced switching has been used but the most successful devices use current in-

duced switching [53]. The array is addressed by x and y conductors. Individual pixels are switched by sending a current pulse to the appropriate x and y lines. The combined magnetic field from both wires is enough to switch the domain. Devices with 48×48 and 128×128 pixels are commercially available from the Semetex Corporation and are being used in a variety of optical processing experiments [3,56,24,29]. The SIGHT-MOD (Semetex Iron Garnet H-Triggered Magneto-Optic Device) is a popular device and it is worth commenting on its characteristics. In its favour is that it is fast. The Litton Corp. has reported continuous frame rates of 1100 frames/s, changing half the elements each time [24]. It has a high contrast ratio of about 1000:1 [53]. It is bistable, so continual scanning is not required. It can be fabricated in relatively large array sizes. A 256×256 laboratory unit has been made [24] with pixel centres separated by 76μm.

The disadvantages of the device include low optical efficiency. Because of the low degree of polarisation rotation, coupled with absorption in the device, the total transmission is only a few percent. Each row and column requires separate addressing wires from an external circuit which supplies short duration current pulses. This becomes ungainly for a large array. Power dissipation is a possible limiting factor for high speed coherent applications. At the frame rate quoted above, the power dissipated in the conductors is about 0.4W/cm^2. This is likely to be sufficient to induce phase distortions across the SLM unless special precautions are taken.

A potential disadvantage for this technology is the difficulty of integrating control circuitry onto the device. This is difficult for two reasons. The first is the problem of integrating circuitry on the magneto-optic substrate, or alternatively of depositing the magneto-optic layer on a conventional integrated circuit. The second difficulty is more fundamental to the modulating material and that is, that to generate, locally at the pixel, the switching currents required by the material is not easy with conventional electronics. The reasons why this consideration may become important are discussed in section 6.3.

Deformable structure spatial light modulators

It is beyond the scope of this thesis to discuss deformable structure SLMs in detail, but there are some recent devices which are sufficiently promising, and relevant to this project, to merit inclusion. The SLMs discussed above can often be configured as either amplitude or phase modulators. The devices described here are all intrinsically phase modulators operating in reflection.

Many phase modulators use mirrors made by depositing a thin metal reflective layer on a flexible substance. The mirror is distorted to form the required phase profile. The distortion can be caused by using electrostatic forces to change the thickness of the flexible layer. This is how the γ-ru icon works; a study of the γ-ruticon is found in reference [36]. Alternatively the flexible structure can be a membrane which is stretched over a pixelated former. The membrane is electrostatically deflected on a pixel by pixel basis. A device of this type is described by Pape and Hornbeck [47]. It uses a nitrocellulose membrane stretched over a silicon chip. The chip has a 128×128 array of electrodes which control the deflection of the membrane. The silicon backplane is similar to those planned for reflection mode FLC SLMs.

The Photo-Emitter Membrane Light Modulator (PEMLM) [22] also uses a thin stretched membrane. The membrane is stretched over the end of a microchannel plate (MCP). The electron "image" emitted by the illuminated input photocathode is amplified by the MCP before the charge image is deposited on the membrane. This device is interesting because the addressing scheme (which is only outlined here) allows certain image processing operations to be carried out on the device. Image addition, contrast enhancement, thresholding and boolean operations have been reported [23]. The practical difficulties involved in the construction of this kind of device are significant. One major problem is that the visible light photocathode is poisoned if it is not kept in an ultra high vacuum. The baking which is required to outgas the apparatus restricts the materials which can be used for the membrane [52].

A promising device developed at Texas Instruments by Wu et al. [67] is the monolithic DMD (Deformable Mirror Device). It incorporates tiny hinged mirrors on a silicon chip similar to the deformable membrane device described above. The mirrors are deflected by voltages read onto underlying electrodes. Small analogue deflections are used in this device. A variant of this is the Bistable DMD reported by Hornbeck et al. [32]. Each mirror is mounted on a micro-mechanical torsion bar and is tilted through a large angle ($\pm 8.9°$) by electrostatic forces. The underlying electrodes can be biased so that the device can operate in monostable, bistable or tristable modes. The controlling voltages are compatible with CMOS circuitry, so there exists the possibility of incorporating logic circuitry around the pixels. In this respect these devices are similar to the liquid crystal over silicon family of SLMs.

1.3 Coherent optical processing

Coherent optical processing exploits the existence of the Fourier Transform (FT) of spatially encoded data in a coherently illuminated optical system to perform image processing functions like image modification and pattern recognition [63]. Figure 1.3 is a schematic of an optical processing system. There are three planes of interest. These are the input plane, the Fourier plane and the output plane. The point source and the collimating lens produce a monochromatic plane wave which is incident on the input plane. The input plane contains the data (image) to be processed. It is presented to the system as a two dimensional (amplitude) transmission function, $t(x, y)$. If the input data contains phase information then $t(x, y)$ is complex-valued. Physically, $t(x, y)$ is realised with some form of spatial light modulator — traditionally a photographic transparency. If, in general, u represents the (scalar) optical field in a plane in the optical system then in the plane immediately to the left of the input plane $u_{ip}^{-}(x, y, t) = Ae^{i\omega t}$, where ω is the (angular) temporal frequency of the optical field ($= 2\pi c/\lambda$) and A is the amplitude of the disturbance (which we can set to unity). The time dependent term can be dropped as it is not observed and does not appear in the subsequent

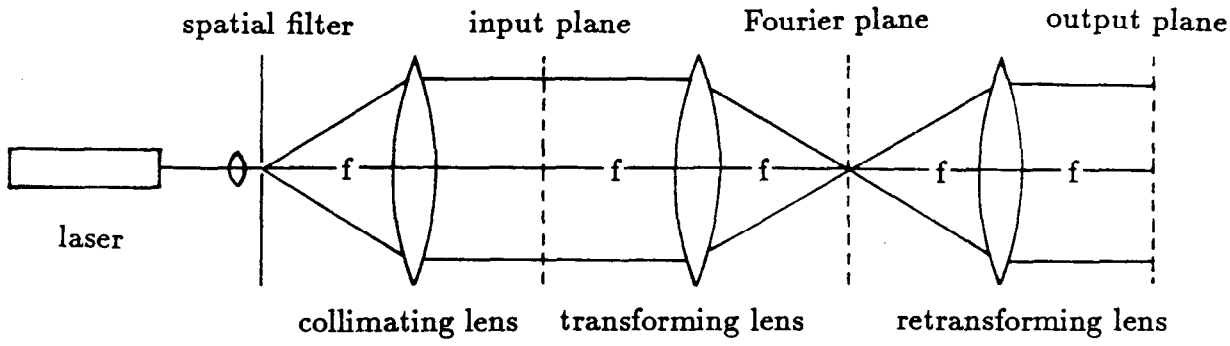

Figure 1.3: The "5-f" optical processor.

discussion. The action of the input-plane spatial light modulator is to multiply u_{ip}^{-} by $t(x,y)$, impressing information on the wavefront so that the field leaving the modulator is $u_{ip}^{+} = t(x,y)$. The first lens forms the Fourier transform of u_{ip}^{+} in its back focal plane — the Fourier plane. [26,63,25].

$$u_{fp}^{-}(s_x, s_y) = \int\int u_{ip}^{+}(x,y) e^{-2\pi i(xs_x + ys_y)} dx dy \tag{1.3}$$

where s_x and s_y are spatial frequency domain coordinates introduced to simplify the notation. The scaling factor between the two coordinate systems is defined such that one "s" unit is the same size as λf "x" units.

As the light crosses the Fourier plane it is multiplied point-by-point by the Fourier plane filter transmission function, $F(s_x, s_y)$. The Fourier plane transmission function is implemented with another SLM, which might be just a mechanical stop or aperture. The light field leaving the Fourier plane is

$$T(s_x, s_y).F(s_x, s_y) \tag{1.4}$$

where $T(s_x, s_y)$ is the FT of $t(x,y)$. The second lens performs a second Fourier transform on this function to yield the output image,

$$t(-x,-y) * f(-x,-y) \tag{1.5}$$

where the $*$ symbol denotes the convolution operation. This is the input image reflected in x and y and convolved with the Fourier transform of the Fourier plane transmission function.

It is pertinent to make some observations about this optical processor at this point in the discussion.

1. The distance between the input plane and the first lens (i.e. f) is chosen to preserve the phase relationship between the centre and the edge of the Fourier transform. If the transparency is moved closer to the Fourier transforming lens then the optical field in the Fourier plane loses the exact FT relationship with the input plane. It appears just the same, but there is a phase curvature imposed on the Fourier transform. For many purposes this is not important.

2. The exact FT discussed above is an idealisation. In practice there are limitations imposed by the optics. Even if we consider aberration-free lenses the finite apertures present in the optics impose an upper limit on the spatial frequencies which are passed by the system. If the spatial frequency limitation of the system as a whole is caused by an aperture *not* in the Fourier plane then the spatial invariance of the FT operation is lost. That is, the spatial frequency components of different parts of the input field have different upper cut-off frequencies.

1.3.1 The effect of using a pixelated SLM in the Fourier plane

Let us consider the use of a pixelated SLM in the Fourier plane of an optical processor as described above. The output image is the convolution of the input image and the FT of the SLM transmission function. To facilitate discussion of the FT of the SLM transmission function it is helpful to use the properties of the Dirac delta function, δ, and the convolution operator, $*$. Consider an SLM

which consists of a square array of pixels all of which are identical and switched "on". We can construct the SLM transmission function as

$$slm(x,y) = rect(\frac{x}{a},\frac{y}{a}) \times [comb(\frac{x}{b},\frac{y}{b}) * pix(x,y)] \tag{1.6}$$

where $pix(x,y)$ is a (possibly complex-valued) function describing the transmission of a single pixel. Figure 1.4 illustrates the construction of the SLM transmission function (in one dimension) and illustrates the notation (which follows Bracewell [10]). Making use of the convolution and similarity theorems the FT of the SLM function is (omitting multiplicative constants)

$$SLM(s_x,s_y) = sinc(as_x,as_y) * [comb(bs_x,bs_y) \times PIX(s_x,s_y)] \tag{1.7}$$

where $PIX(s_x,s_y)$ is the FT of the pixel function $pix(x,y)$. The terms can be easily identified with the properties of the SLM. Inside the square brackets there is the $comb(bs_x,bs_y)$ function. The separation of these δ functions is inversely proportional to the pixel centre to centre distance. This *comb* function samples $PIX(s_x,s_y)$, the FT of the pixel function. $PIX(s_x,s_y)$ is (approximately) the envelope of the entire $SLM(s_x,s_y)$ function. If, for example, the pixel function is $rect(\frac{x}{c},\frac{y}{c})$ which represents a clear square pixel in an opaque background then the envelope is the $sinc(cs_x,cs_y)$ function.

A familiar special case is illustrated if the pixel function $pix(x,y) = rect(\frac{x}{b},\frac{y}{b})$, ie. the "pixels" fit together and occupy the entire area of the array. The SLM is now just a clear window and the term in square brackets collapses to a single δ function. All the δ functions except the central one fall on zeros of the FT of the pixel function.

The term in square brackets is convolved with the "narrow" *sinc* function, $sinc(as_x,as_y)$. Physically this function corresponds to the diffraction from the finite (square) aperture of the SLM. If we consider the special case of the clear-square-window discussed above, then the FT of this SLM is simply this *sinc* function. If this SLM was placed in the Fourier plane of an optical processing system then the spatial frequency cut off is defined by the edge of the window in the Fourier plane. The SLM is a low pass filter which gives the optical system

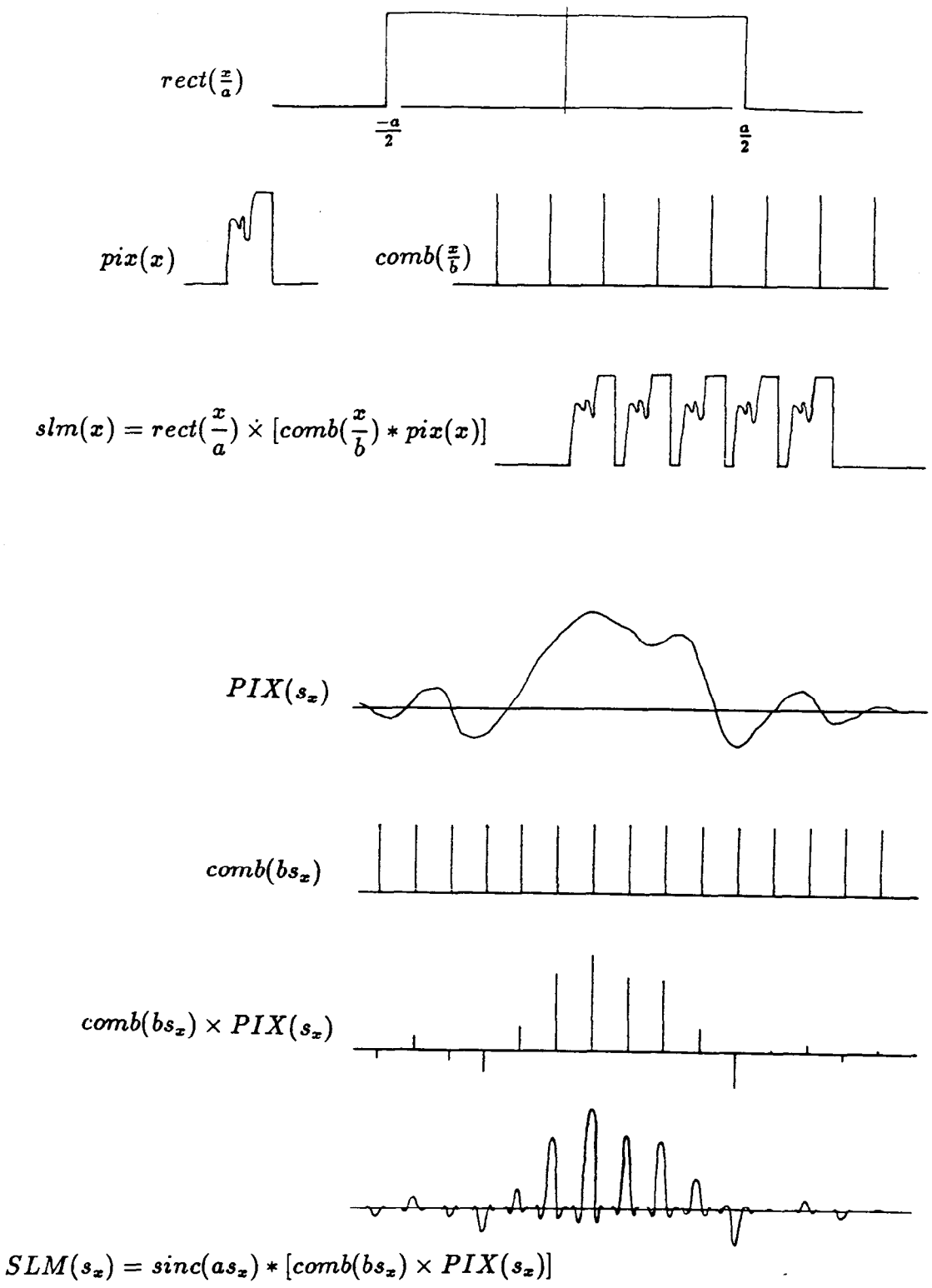

Figure 1.4: The construction of the SLM transmission function; $slm(x)$. The top part of the diagram illustrates the use of the *comb* function and the bounding *rect* function to replicate the *pix* function an appropriate number of times. The bottom part of the diagram illustrates the construction of the FT of $slm(x)$; $SLM(s_x)$. The narrow *sinc* function which is convolved with the modulated *comb* function is the FT of $rect(\frac{x}{a})$ and corresponds to blurring due to the finite size of the (square) aperture.

a point spread function (PSF) of $sinc(ax, ay)$. In this case the "convolution of the input image with the FT of the SLM function" is just another way of saying that the output is blurred by the loss of high spatial frequency information.

Consider now the general pixelated filter where the square brackets contain the sampled FT of the pixel function. Convolving this with the "narrow" *sinc* function replicates this *sinc* function at each point in the δ function array with an amplitude, and phase, determined by the FT of the pixel function. Convolving the input image (complex-amplitude) with this function, yields an output image which is the input image replicated at each δ function, blurred by the "narrow" sinc function and with a complex-amplitude proportional to the FT of the pixel function at that site. Of course, it is the intensity that is observed so the relative intensities of the replicas are deduced from the squared modulus of the pixel function FT.

The implications of using a pixelated Fourier plane filter can now be addressed. Clearly for a given optical system there is a maximum input image size which, if exceeded, causes the output replicas to overlap. There is also a spatial frequency cut-off imposed by the SLM which limits the resolution in the images passed by the system. (Let us assume that the limitations imposed on the system are due to the limitations of the SLM and not by lens apertures etc.) These two limits are in fact manifestations of the same phenomenon. There is a fundamental trade-off between image size and resolution which happens because the FT is *sampled* by the SLM. To illustrate this we can consider how we configure the system firstly to pass larger images and secondly to achieve higher resolution.

To increase the separation of the output replicas we have to decrease the spacing of the pixels in the s coordinate system in the Fourier plane — that is, increase the Fourier plane sampling rate. Given that the SLM is likely to be fixed in size and pixel spacing, the way to do this is to increase the focal length of the lenses. This makes the FT larger. On the other hand, if we wish to pass higher spatial frequencies through the restricted aperture of the SLM, we should use shorter focal length lenses to make the FT smaller — increasing the Fourier plane pass

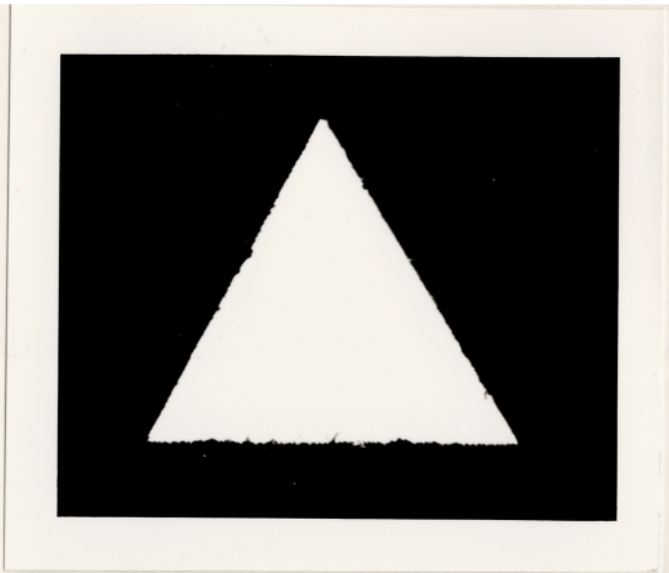

Figure 1.5: The test object with no Fourier plane filtering or sampling. Any loss of resolution is caused by the limited pass band of the optics. These photographs were taken by placing a camera body with the film plane lying in the output plane of the Fourier processor. Ilford HP5 film was used and developed normally with Ilford ID-11.

band.

The product of the Fourier plane sampling rate and the Fourier plane pass band is fixed. It is equal to the number of pixels across the SLM.

The effect of sampling in the Fourier plane is illustrated in figures 1.5 to 1.10. These photographs were prepared on a modified form of the optical bench which was used for the SLM experiments and which is described in section 5.1. The test input image was a triangular aperture in an opaque material. This kind of object is free from the possibility of the phase gradients which are often found on photographic film at high contrast edges. Sampling and band limiting in the Fourier plane were done with small metal grids and apertures. The photographs are of the output of the optical processor, with Fourier plane sampling rates and band limits which mimic the electronically addressed SLMs which are described later.

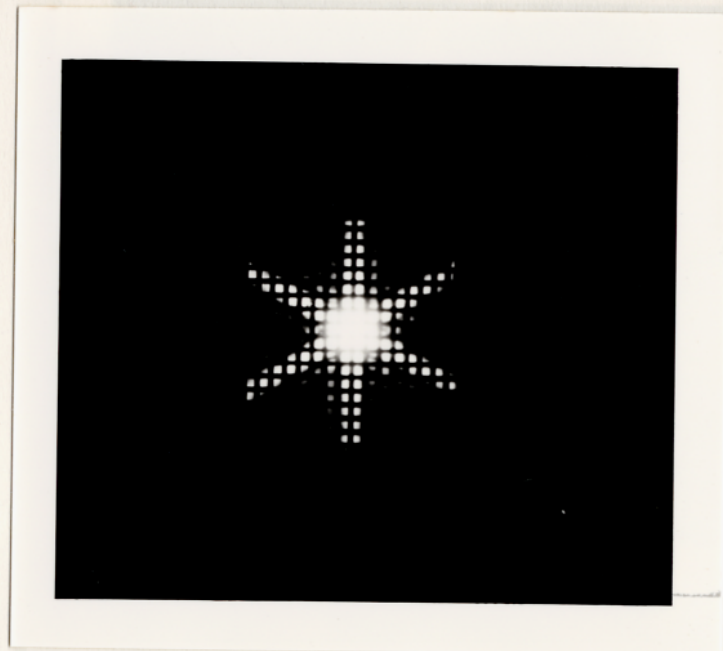

Figure 1.6: This figure shows the Fourier plane being sampled by the 16×16 grating. The scale of the FT has been arranged to give the optimum sampling rate — the output images are as large (and detailed) as possible without overlapping; see the next figure.

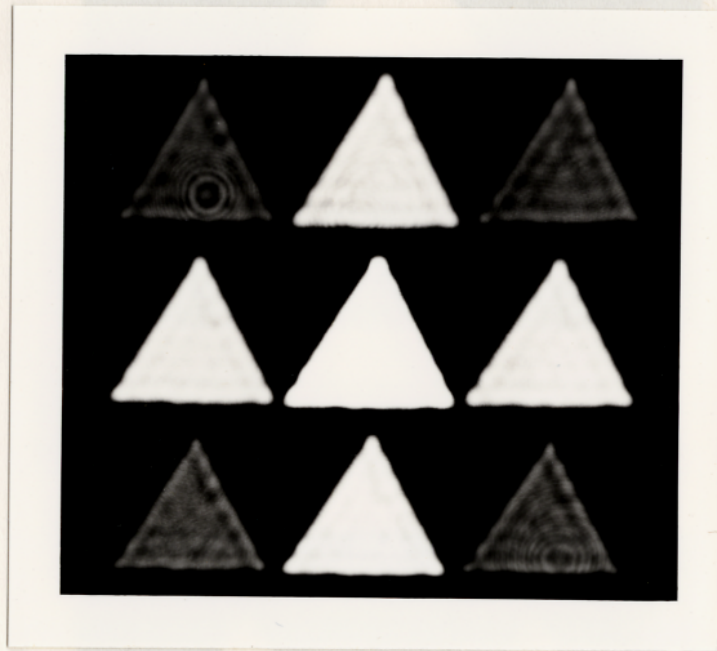

Figure 1.7: This figure shows the output image when the FT is sampled as shown in the previous figure. The output replicas are just separated, indicating optimal sampling. The rounded edges and the "ringing" that are characteristic of a sharp high frequency cut-off are visible.

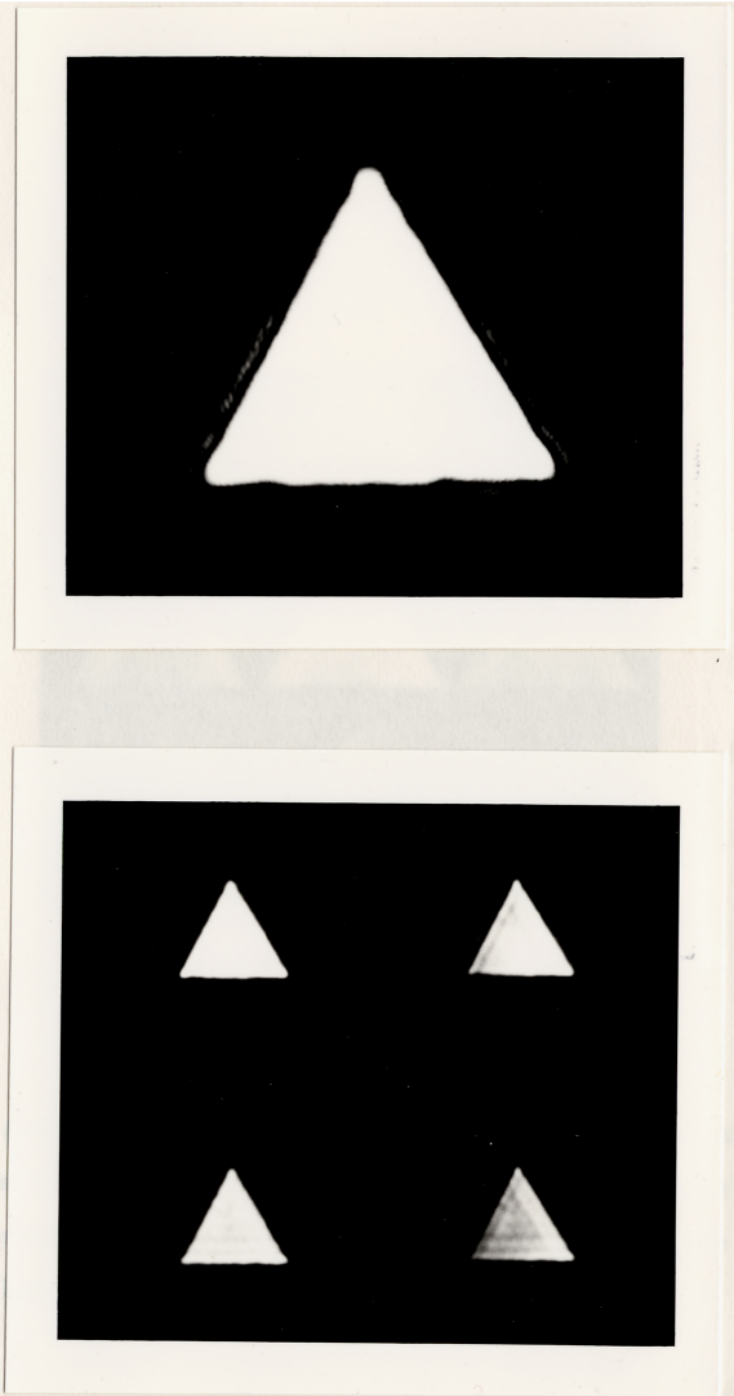

Figure 1.8: The Fourier plane has been sampled by a 50×50 grating. The pass band has been kept the same as for the 16×16 filter, so the sampling rate is higher. This separates the output replicas more widely. Shown here are photographs of one of the output replicas for comparison with the 16×16 example, and of a larger area of the output field to illustrate the increased separation of the replicas.

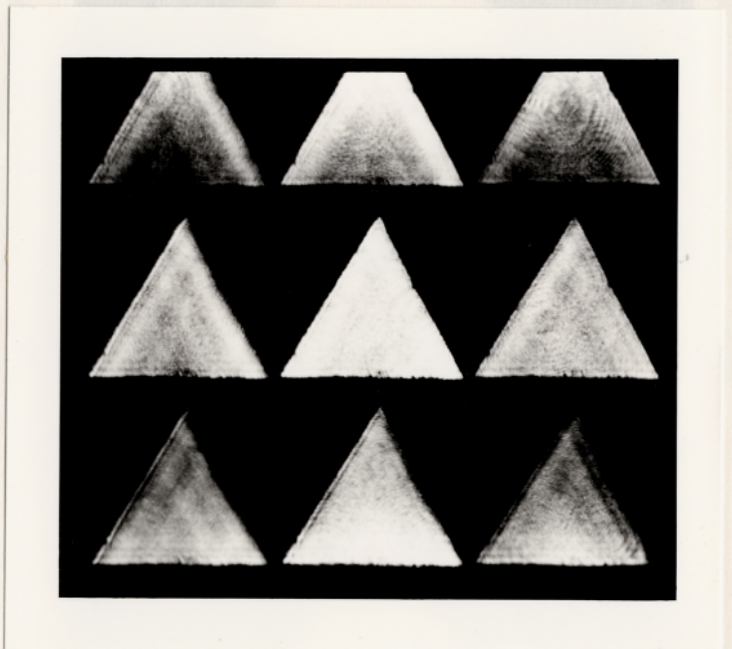

Figure 1.9: The scale of the FT has been changed to exploit the larger number of samples available with the 50×50 grating. The FT has been made smaller so allowing higher spatial frequencies through the aperture. The output images are now closer together and have better resolution.

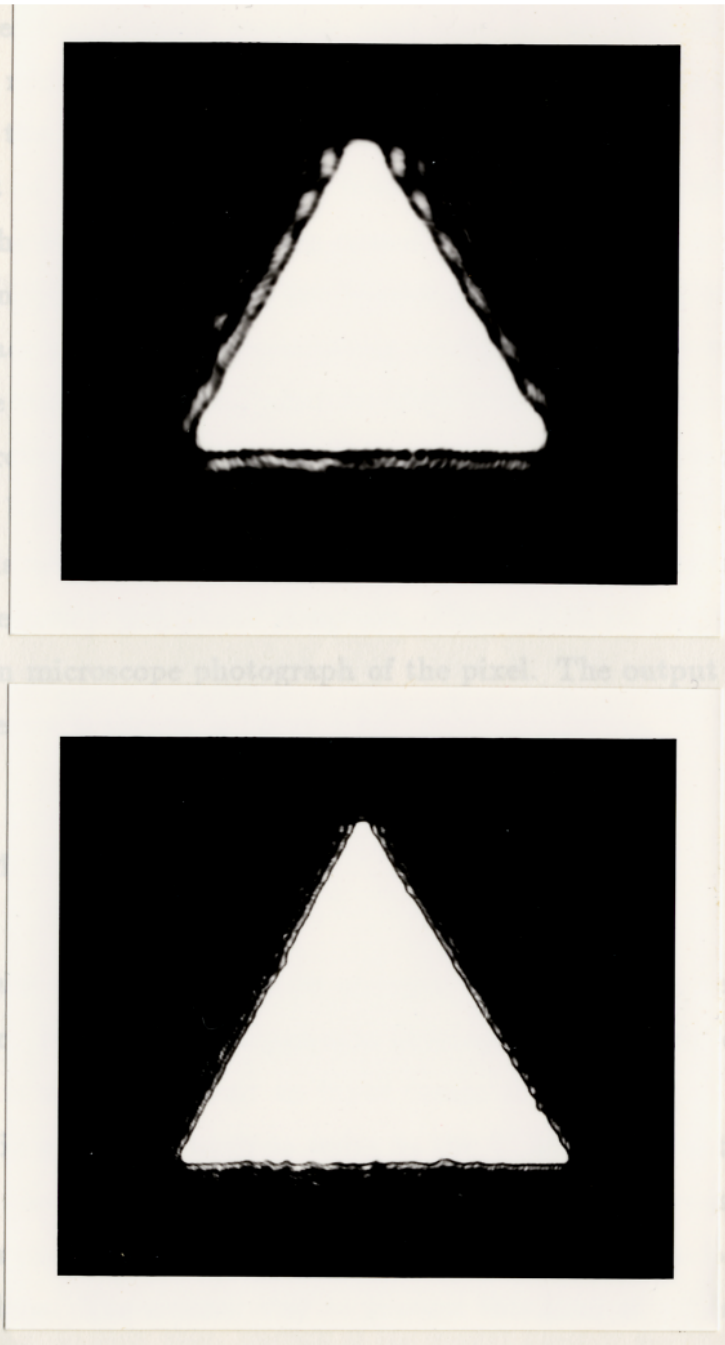

Figure 1.10: As an illustration of the different pass-bands available with these array sizes, the gratings were replaced with an adjustable aperture. Pass-band limits were applied by setting the size of the aperture in the Fourier plane. The top photograph is of the triangle with the pass band set at the optimum for a 16 × 16 grating with this size of object. The photograph on the bottom was taken on the same optical system, except the pass band is increased to simulate the pass band of a 50 × 50 array.

In these examples transmission gratings were used in the Fourier plane. The gratings did not match each other for mark to space ratio or even in the shape of the pixels — the 50 × 50 grating had slightly rounded pixels. As has been stated the effect of changing the pixel function is only to change the energy distribution in the output, the blurring caused by the small number of samples is the same for any pixel function. If the Fourier plane filter is implemented with a reflecting surface instead of a transmitting surface then the above arguments still hold. Phase variations in the pixel function now correspond to changes in "height" of the reflecting substrate. To illustrate the effect of a complex-valued pixel function a bare 50 × 50 SLM chip was used as a reflecting Fourier plane filter. The pixels are essentially identical to each other but they have quite a complicated reflectivity and phase structure. Figure 3.12 on page 97 shows a scanning electron microscope photograph of the pixel. The output image from the optical processor is shown in figure 1.11.

Pixelated SLMs in the input plane

It is possible to use a pixelated SLM as an input device for a Fourier transform optical processor. Many of the arguments developed above carry over to this case. The SLM is used to present an input image to the system. This image may already be in a suitable form to write to the SLM. If it is not it must be sampled to suit the pixel array. When the image is Fourier transformed the pixelation causes the spectrum of the (unsampled) input image to be replicated in the Fourier plane. The normal way to process this kind of FT is to allow a single spectrum through the Fourier plane. By operating on only one spectrum the Fourier plane SLM is used most efficiently. Its limited number of pixels is not wasted processing information that codes only the pixelated nature of the input plane. The finite number of samples causes *aliasing*, i.e. the high spatial frequency part of the individual spectra overlap and cannot be used. Of course this is just another way of saying that one cannot write more detail onto an SLM than there are pixels available.

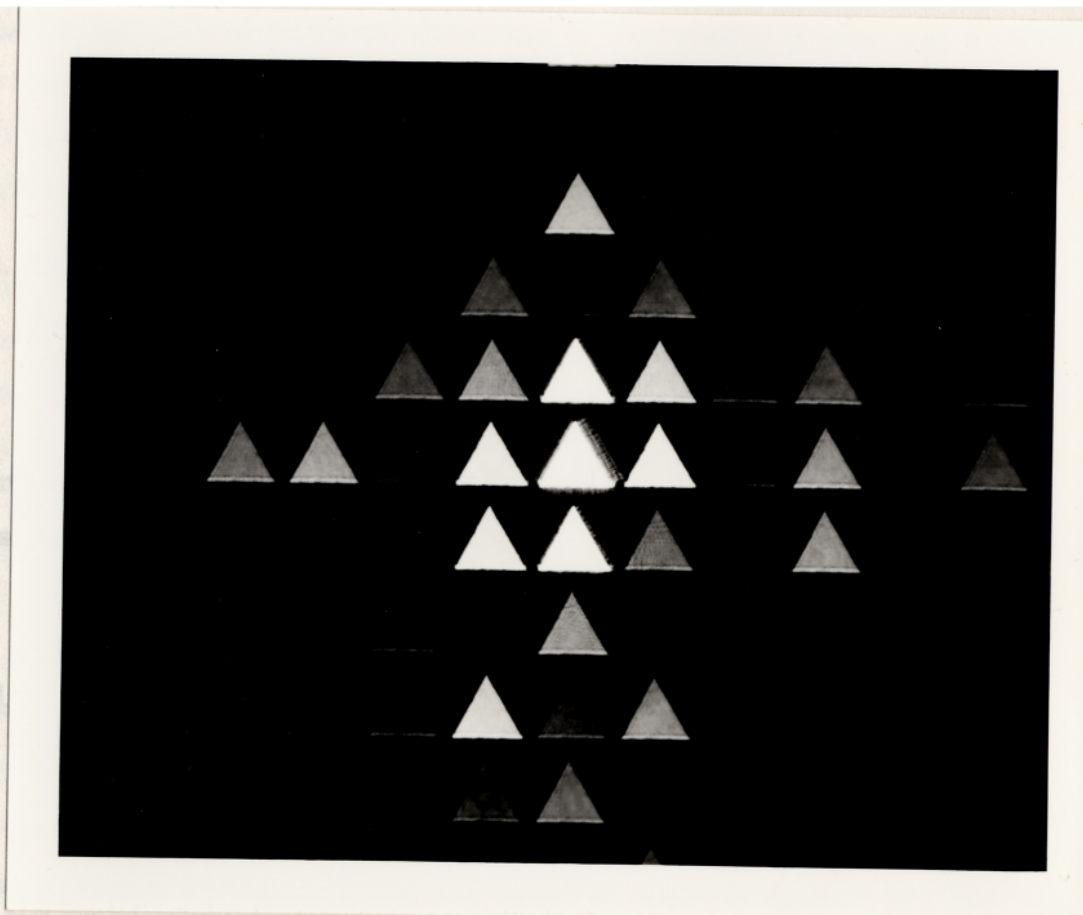

Figure 1.11: The output of the optical processor when the Fourier transform is reflected from a bare 50×50 SLM chip. Enough of the output plane is shown to illustrate the asymmetric nature of the output field. This is a consequence of the complex nature of the pixel function.

The theoretical discussion of pixelated SLMs has implications for the design of practical devices. In summary, we can say of pixelated SLMs in Fourier transform optical systems that;

1. The number of pixels on the device is important. A pixelated SLM is intrinsically a low-pass filter because of the limited number of samples that is taken. The size of the SLM is not important, other than for convenience in the optical system design.

2. The form of the pixels is not important. The reflective area of the pixels does not have to be square, or even flat. The important thing is that all the pixels should be identical.

There are, however, other factors involved in the design of a practical device. These are discussed in chapter 3, section 3.1.

1.4 Incoherent optical processing

The spatial light modulator described in this thesis is intended primarily for coherent optical systems. There are, however, some incoherent applications which are possibly suited to this type of SLM. Attempts are being made to use the connectivity and parallelism available in optical systems to solve certain specialised computing problems. One of the areas which may benefit from an optical approach is neural computing.

Parallel neural computing

Artificial neural networks are recognised as being potentially useful in applications such as content-addressable storage, error-correction coding and optimisation computing [49,38,31] so there is some motivation to develop efficient hardware implementations of these processing architectures. Neural networks require

highly interconnected but simple processors. The kind of operation required at a "neuron" is a sum over many inputs followed by a thresholding process. The result of the thresholding becomes the output of that neuron. The inputs to the neuron are weighted outputs from all, or many, of the other neurons. The process is repeated for many iterations. There are several different types of neural network, but they share the properties of being robust against individual neuron failure, of requiring high levels of interconnection and of benefitting from a high degree of parallelism in the computation.

Psaltis and Farhat et al. [49,19] have implemented a fully connected (Hopfield) neural net based on an optical vector-matrix multiplier. The vector-matrix multiplier uses cylindrical lenses to broadcast a signal from one of a row of light emitting diodes (LEDs) onto a column of a mask. Light emerging from the other side of the mask is imaged in such a way that all the light from one row is integrated onto a single photodetector. The vector elements are the "neurons" and the matrix (mask) elements form the interconnection weights. Psaltis and Farhat have used binary valued masks in an incoherently illuminated hybrid system. Electronic thresholding was used in this experiment. The information stored in the network is distributed among the connection matrix elements. An adaptive SLM is particularly suitable for the function of the mask.

More recent experiments have concentrated on all-optical systems using volume holographic interconnection matrices. The function of a SLM in this kind of system is as an input device for programming the network.

Signal switching

The interconnection power of optics holds the potential to realize reconfigurable multiple communication paths between processing elements. This will probably be implemented in some form of crossbar switch. An $n \times n$ crossbar switch can reconfigure the connections between any m ($m \leq n$) transmitting ports and any k ($k \leq n$) receiving ports in such a way that changing one connection will not

affect any of the others. The crossbar can be implemented in the same way as the matrix multiplier described above. Each pixel in the SLM corresponds to a connection between an input and an output port. Note that one transmitter can broadcast to many receivers. The paper by Neff [46] describes this application in the context of a general discussion of hybrid electronic/optical computing.

Digital optical logic

There are techniques by which Boolean operations can be applied to optical images. The aim is to design massively parallel computers which perform, simultaneously, simple operations on large arrays of data (images). In the shadow-casting system of Tanida and Ichioka two input data planes are encoded and presented to the system in the form of pixelated masks. LEDs illuminate the masks and a decoding mask enables the results of all sixteen possible logic functions to be extracted. The method is extensively developed in three papers [57,58,59] which describe the principle of operation of an optical parallel array processor (OLAP).

Johnson et al. [35] and others [60,68] have encoded binary logic levels in the polarisation state of a light beam. This has advantages over intensity based "bright" and "dark" logic when XOR or XNOR functions are required. Electrically addressed ferroelectric and nematic LCs have been used in modulating arrays, operating either as switched wave plates (FLCs) or in a twisted nematic mode (nematic LCs, see chapter 2).

1.5 The objectives of this project

The research by Ian Underwood at the University of Edinburgh [61] was aimed towards constructing a spatial light modulator by coupling the relatively mature technologies of integrated circuits and liquid crystals. This work resulted in a

working low resolution (16 × 16) prototype SLM. The aim of this project is to use "state of the art" microelectronic technology to construct a more useful SLM and to investigate the problems associated with the use of small geometry electronics in SLM applications.

An outline of this thesis

Chapter 2 contains an introduction to liquid crystals followed by a description of some light modulating LC configurations. Results from test cells are presented. A test SLM using the hybrid field effect in a nematic liquid crystal on a 16 × 16 silicon backplane is evaluated.

Chapter 3 introduces integrated circuit technologies and describes the design and process parameters of the Edinburgh 1.5μm nMOS process. The overall layout of the chip and the overall structure of the SLM circuit are described. The SLM circuit is described in some detail and design strategies are discussed.

Chapter 4 contains the results of the electronic testing of the circuits. The detailed behaviour of some circuits is explored and operational limits are found.

Chapter 5 begins with a description of how the SLM was constructed. There follows a description of the optical system used to evaluate the SLM in some simple optical processing experiments. Results from these experiments are presented. In the concluding chapter the performance of the SLM is assessed, and an attempt is made to address the issues concerning the future of this approach to SLM design.

Chapter 2

Liquid Crystals for Spatial Light Modulators

2.1 An introduction to liquid crystals

The term *liquid crystal* is applied to the intermediate phases (mesophases) that occur between the solid and the isotropic liquid phases of certain organic materials. They are intermediate in the sense that while retaining some of the properties of liquids — such as flowing easily — they retain some of the symmetry properties of crystals. The liquid crystals which will be discussed here are also intermediate in the sense that, for these materials, the mesophases occur only in a range of temperatures between the solid and the conventional liquid phases. This kind of mesophase is called *thermotropic*.

Liquid crystal mesophases occur only in materials which have "strongly elongated" molecules [16]. This characteristic rod shape is often formed by linking aromatic rings with hydrocarbon chains. Other chemical groups, substituted onto the chains, cause some of the interesting properties of the materials. The usefulness of these mesophases comes from the associated anisotropies in other macroscopic physical properties, particularly the refractive index and dielectric anisotropies. The refractive index anisotropy can be used to modify the polarisation state of a light beam, and the dielectric anisotropy gives a method of reorienting the axis of the optical anisotropy in the fluid. The popularity of

liquid crystals as a modulation medium stems from the fact that the relatively large optical anisotropy can be controlled by a low voltage, because of the weak restoring forces in the liquid crystal mesophase. Unfortunately a consequence of the mechanism which allows low voltage modulation (ie. the weak restoring forces) is a fairly slow response time.

The rest of this section contains a description of some of the liquid crystal effects used for light modulation with the emphasis on the effects which are suitable for use in a spatial light modulator. A detailed exposition of the liquid crystal mesophases is given by deGennes [16]. The book by Blinov [8] puts more emphasis on the electro-optic effects in liquid crystals.

2.1.1 Liquid crystal mesophases

It is usual to classify liquid crystals into three groups: nematic, cholesteric and smectic. The smectic phase is further divided into subclasses A,B,C...K, [8] referred to as smectic-A (or S_A) etc. The structures of these groups are illustrated schematically in figure 2.1. In the discussion of the liquid crystal mesophases it will be useful to refer to the *director*. The director is a (unit) vector which specifies the local average molecular orientation.

Nematic liquid crystals are characterised by the existence of an orientational order, and the lack of any translational order, of the molecules in the liquid. In the absence of external forces the molecular interactions favour locally parallel alignment, though not in any particular direction. A bulk sample has an opaque appearance caused by spatial and temporal fluctuations of the director, which cause light to be scattered by the associated fluctuations of the refractive index. Thin samples can be aligned to form transparent birefringent mono-crystals.

Cholesteric liquid crystals have been identified as a variant of the nematic mesophase [16]. Locally the structure of a cholesteric is similar to that of a nematic. The difference is that the average orientation of the director is not

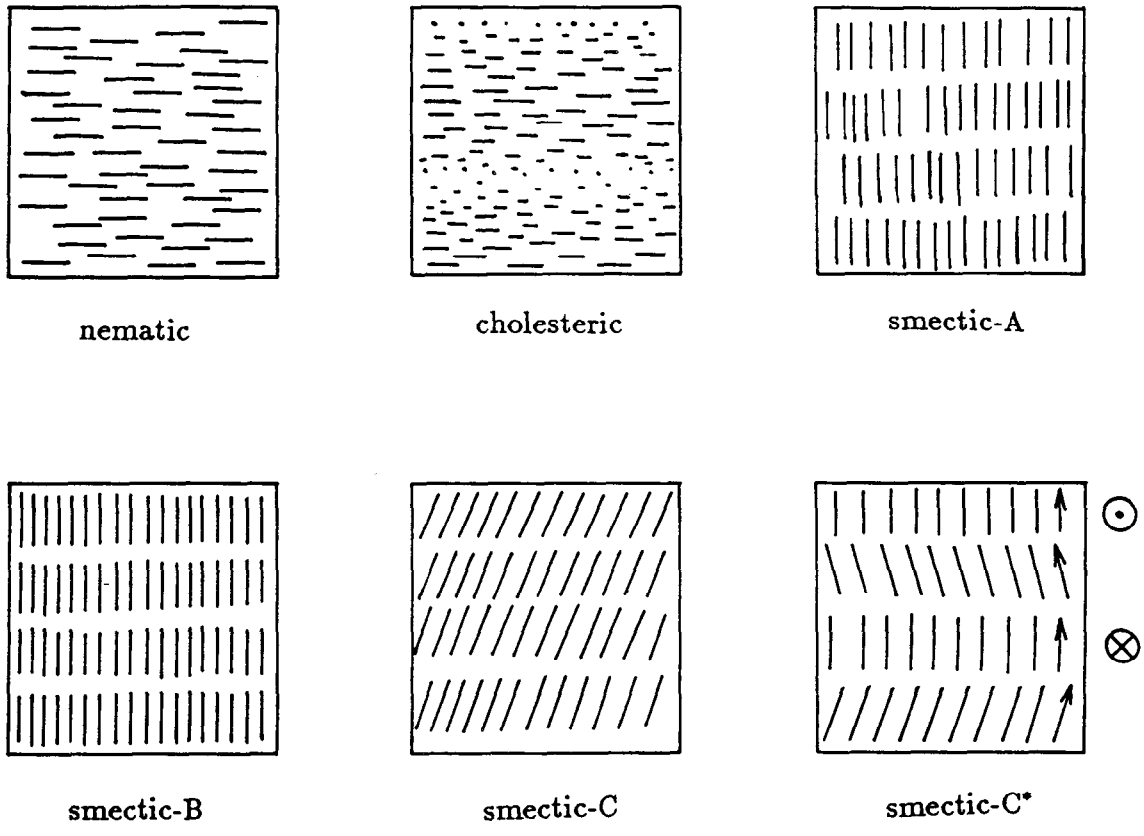

Figure 2.1: Liquid crystal mesophases. The smectic mesophases have varying degrees of positional order as well as the orientational ordering that is found in the nematic and cholesteric mesophases. S_C has the same translational order as S_B but the molecules are tilted with respect to the layer normal. In S_C^* the direction of tilt precesses from layer to layer. In the diagram, the layers which slope into and out of the page are indicated by the vector "head" and "tail" symbols.

constant throughout the sample. The preferred configuration, illustrated in figure 2.1, is helical. The pitch of the helix is of the order of the wavelength of light. This is exploited in some display applications. It is reasonable to consider the nematic as a special case of the cholesteric mesophase with infinite pitch. As in nematics there is no translational ordering in the cholesteric mesophase.

Smectic mesophases have a higher degree of ordering than nematics: in addition to orientational order they all have layered structures, and so have some level of

translational order. The least ordered is S_A, which has essentially no correlation between molecular positions on the different layers. One of the most interesting from a device point of view is the ferroelectric chiral S_C phase (S_C^*). It is beyond the scope of this thesis to discuss S_C^* liquid crystals in much detail. They are the subject of much current research by Crossland et al., Patel and Goodby, Johnson et al. and many others [9,48,34]. The S_C^* structure is similar to S_C which is layered and has translational ordering, like S_B, but which has the director tilted from the layer normal. The chirality manifests itself as a precession of the direction of tilt of the successive layers, see figure 2.1. The director lies on the surface of a cone. It is possible to suppress the helicity, for example by surface forces, and constrain the director to lie in one of only two orientations. The liquid crystal can be switched between these two stable orientations by a dc pulse. The change in the direction of the optic axis can be used to modulate light, with a suitable polariser configuration. The modulation is achieved by a pure rotation of the molecules, thereby avoiding the back-flow found in most nematic switching [8]. These devices switch faster than nematics, typically in tens of microseconds rather than tens of milliseconds.

2.1.2 Modulating light with nematic liquid crystals

We shall consider further the modulation of light with nematic structures. In a bulk sample the material is opaque in appearance because of inhomogeneities in the refractive index of an unaligned sample. The liquid crystal can be uniformly aligned in a thin sample by constraining the orientation of the molecules at the walls of the sample — often parallel to the walls and with a known direction. The result is a uniaxial mono-crystal. The birefringence (Δn) of the material is quite high (BDH mixture E7 has $\Delta n = 0.225$ [1]) so cells have to be only a few microns thick to perform useful optical modulation. The construction of a typical LC test cell is shown in figure 2.2.

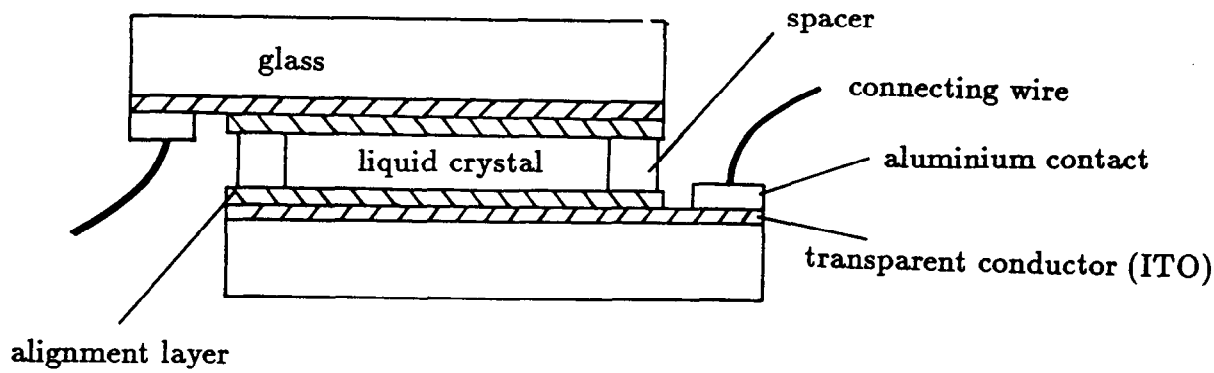

Figure 2.2: A typical LC test cell. The transparent conductor is a layer of sputtered Indium-Tin Oxide (ITO).

Alignment of liquid crystals

There are two basic forms of LC alignment — homogeneous and homeotropic. In a homogeneously aligned liquid crystal the director is constrained to lie parallel to the walls of the cell by an appropriate surface treatment. This usually involves rubbing the coated glass substrate with cloth or tissue, or obliquely evaporating magnesium fluoride or silicon monoxide onto the substrate. The alignment mechanisms are not well understood; for a discussion of them see the paper by Castellano [12]. Homeotropic alignment, in which the director lies perpendicular to the substrate, can be obtained by coating the glass with a suitable surfactant, e.g. lecithin. Homogeneous alignment is required for most light modulation applications.

Dielectric anisotropy

The static dielectric constants of the LC, $\epsilon_{\|}$ and $\epsilon_{\perp}$ (measured parallel and perpendicular to the director), are different. If $\epsilon_{\|} > \epsilon_{\perp}$ the the material is said to have a positive dielectric anisotropy (PDA), otherwise it has a negative dielectric anisotropy (NDA). The magnitude of the dielectric anisotropy depends on the detailed structure of the constituent molecules. It is the sign of the dielectric anisotropy that determines how the liquid crystal reorients in the presence of an electric field. A PDA nematic tends to align parallel to the field.

Light modulation effects

Some of the liquid crystal effects which have been used in displays are inappropriate for spatial light modulation, either because of low contrast or because of phase disruption. One LC display effect which could be suitable for SLMs is the *twisted nematic* (TN) effect. The principle of operation is illustrated in figure 2.3. A homogeneously aligned cell is prepared with an angle, of usually 90°, between the alignment directions on the glass plates. The nematic takes up a

twisted structure. The light modulation effect relies on the polarisation guiding property of a twisted uniaxial structure. If the pitch of the resulting helix is large enough to satisfy Mauguin's condition [8] then the polarisation plane of light, incident with its plane of polarisation aligned parallel (or perpendicular) to the director on the front surface, emerges rotated by the twist angle of the cell. If a PDA liquid crystal is used, then a voltage between the transparent electrodes on the glass plates will tend to realign the liquid crystal molecules perpendicular to the cell walls. Usually an ac signal is applied because a dc bias tends to shorten the life of the LC by inducing electrochemical degradation (probably at the bounding layers [15]). As the voltage is increased and the tilt angle of the molecules in the centre of the cell increases, it becomes energetically more favourable for the twist to unwind in the layers near the cell walls. The "twist" is now concentrated near the centre of the layer but is unobservable because of the homeotropic alignment. The polarisation plane is not rotated by the cell and the light is passed (or blocked) by an analyser. The TN effect is used in LC TV displays because it has quite good contrast, response speed, and multiplexibility[1]. It is not suitable for a reflection mode device unless an analyser is incorporated between the cell and the reflector. This is not convenient in the envisaged use where mirrors on an IC are used as reflectors *and* as LC driving electrodes. The 90° twisted structure can be impaired by regions of reverse twist — ie. areas of the cell where the helix has taken the opposite handedness. The symmetry of the boundary conditions can be removed by anchoring the molecules to the walls with a small amount of pre-tilt. Or the symmetry in the nematic structure can be broken by the addition of a small amount of chiral dopant. The pre-tilt favours one helicity by reducing the strain energy associated with it, compared to the one with the opposite handedness. The chiral dopant makes the nematic behave like a cholesteric with a large pitch. This "weak" cholesteric favours one handedness of helix.

The twisted nematic effect is almost exclusively used in amplitude modulators

[1]The size of array that can be addressed with multiplexed row and column wires depends on the steepness of the optical response to voltage signals. This is sometimes referred to as the multiplexibility of the configuration, see section 1.2.2 or reference [45].

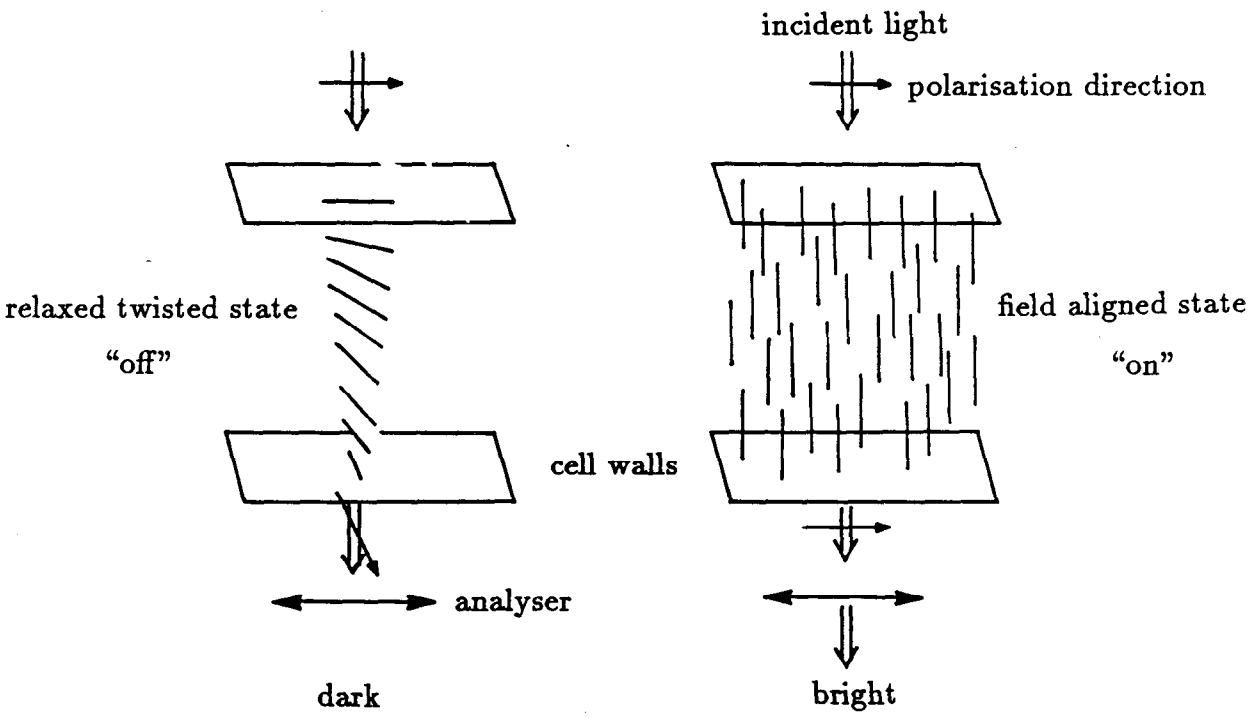

Figure 2.3: The twisted nematic effect. The analyser can be aligned to make either state transmit. In the relaxed (0V) state the deformation is one of pure "twist". The director is parallel to the cell walls, ie. there is no "tilt".

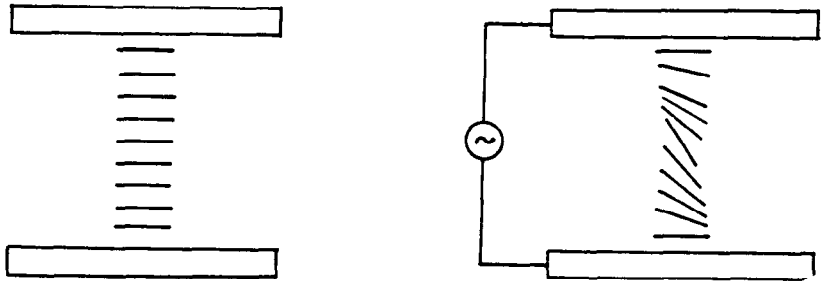

Figure 2.4: The voltage controlled birefringence mode. This can perform pure-phase modulation. Light polarised with its electric vector parallel to the page would experience a reduced path length on traversing the cell on the right.

operating in transmission mode. A similar structure can be used in reflection or transmission, for phase modulation. This is called the *voltage controlled birefringence* (VCB) mode. The cell is arranged as a parallel nematic monocrystal by aligning the directors at both walls to be parallel with each other — an untwisted nematic. In the "off" state, light incident on the cell polarised parallel to the director will experience an optical path length equal to $n_e.t$ where n_e is the extraordinary refractive index of the LC and t is the cell thickness. As the cell voltage is increased past the Frederiks threshold [16,8] the molecules begin to tilt, figure 2.4. The refractive index ellipsoid tilts with them, so the light passing through the cell experiences a reduced refractive index and a correspondingly reduced optical path length. A double pass in a reflection system enhances the phase modulation. This effect has been used by Ranshaw [50] who used a 16×16 IC backplane [62] to control the LC. This configuration can be used in a reflection device as an amplitude modulator by orientating the director at 45° to the polarisation plane, and analysing the resulting elliptically polarised light.

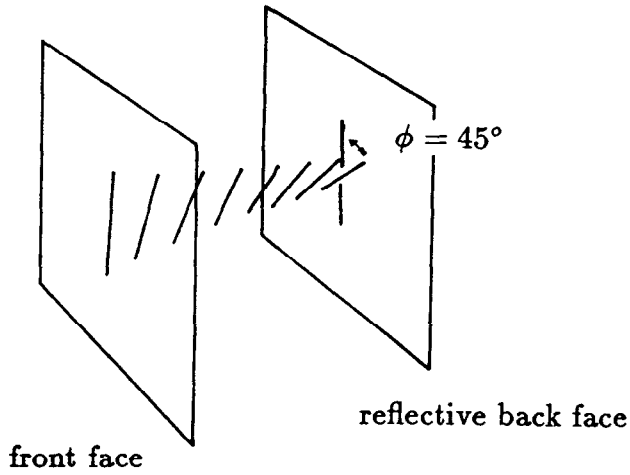

Figure 2.5: The LC configuration used in the hybrid field effect.

For amplitude modulation in a reflection mode device the *hybrid field effect* [28] appears to have some advantages over the voltage controlled birefringence effect. The hybrid field effect uses a 45° twisted nematic structure. The "off" state occurs when the nematic structure is relaxed. The twist guides the input polarisation plane through 45°, the light is reflected from a mirror/electrode, and as it propagates back through the cell the polarisation plane is rotated back to its initial orientation. Usually a beam splitter is used to reflect the output beam through an analyser which is set to block out this polarisation state. To switch the cell "on", an ac signal applied to the electrodes realigns the molecules in a way similar to the voltage-realigned twisted nematic. The twist tends to concentrate in the middle of the cell where the director is tilting towards the direction perpendicular to the cell walls, see figure 2.5. Because of the tilt in this region, the liquid crystal does not appear strongly birefringent, and so the polarisation guiding begins to break down. The thin layer of liquid crystal next to the reflecting electrode has less tilt than the material in the centre of the layer and so is still quite strongly birefringent. The direction of polarisation of the light is not aligned with the optic axis of this birefringent layer, so the double propagation through this layer causes the polarisation state

to become elliptical. As the light traverses the birefringent layer close to the front surface, for the second time, the polarisation state is altered more. The detailed behaviour is complicated and is examined theoretically by Montgomery in papers on the "off"-state [43], and the "on"-state [44] of this configuration. It was decided to use the hybrid field effect as the liquid crystal configuration in the IC addressed SLM.

The advantage of the hybrid field effect over the voltage controlled birefringence effect is that it is less sensitive to thickness variations in the LC layer. The "off" state is produced primarily by polarisation guiding, and so is more uniform than the VCB "off" state for a given thickness variation. There is a phase variation introduced along with the amplitude modulation. It is, in general, difficult to produce grey-scale pure-amplitude modulation with liquid crystals. The problem is circumvented in a binary device where, if the contrast ratio is high, the phase of the "off" state can be ignored.

The liquid crystal effect that was used by Underwood in the prototype amplitude modulating IC addressed SLM [61] is the *guest-host* effect. A dichroic dye (the guest) is added to a nematic LC (the host). The resulting "liquid polaroid" can be realigned in the usual way, allowing the absorption of polarised light to be controlled. Though the contrast ratio available from the liquid crystal itself is quite good, the contrast which was obtained from the SLMs was poor. The principal reason for this was that there was a constant background intensity reflected from the air/glass and glass/ITO/LC interfaces. The "off" state was washed out by this light. The hybrid field effect uses a crossed analyser which blocks the front face reflections.

2.2 Experimental investigation of the Hybrid Field Effect

The hybrid field effect was investigated experimentally to assess its suitability for use in an IC addressed SLM.

2.2.1 The liquid crystal test rig

An optical bench was assembled to evaluate the LC configuration under conditions similar to the intended use in the SLM. A schematic of the liquid crystal test bench is shown in figure 2.6. Helium-neon (633nm) lasers were used in all the optical experiments described in this thesis. The laser illumination is incident normal to the cell with its plane of polarisation oriented as shown in the diagram. This direction was chosen to prevent the beam splitter introducing a degree of ellipticity in the light returning from the test cell in the "off" state. This would reduce the measured contrast ratio as it is strongly dependent on the "off" state intensity. A photodiode/amplifier chip (Centronics OS15) was used to detect the output from the LC cell. The output voltage of the photodiode chip was fed through a variable gain, dc-coupled, amplifier and filter circuit to the analogue input port (ADC) of a BBC microcomputer. The microcomputer set the amplitude of the ac signal to the LC cell, waited during a "settling time" (about 1s) and then recorded the voltage on the analogue input port. The measurement and control apparatus is similar to that used by Vass et al. [64]. The system allowed easy, automated data collection. Some points should be made concerning the LC testing:

1. Great care was taken to measure accurately the "off" intensity as this measurement is crucial to the specification of the contrast ratio.

    - Melles Griot sheet polaroids were used. Two were selected which gave the best extinction ($> 3000 : 1$ in intensity).

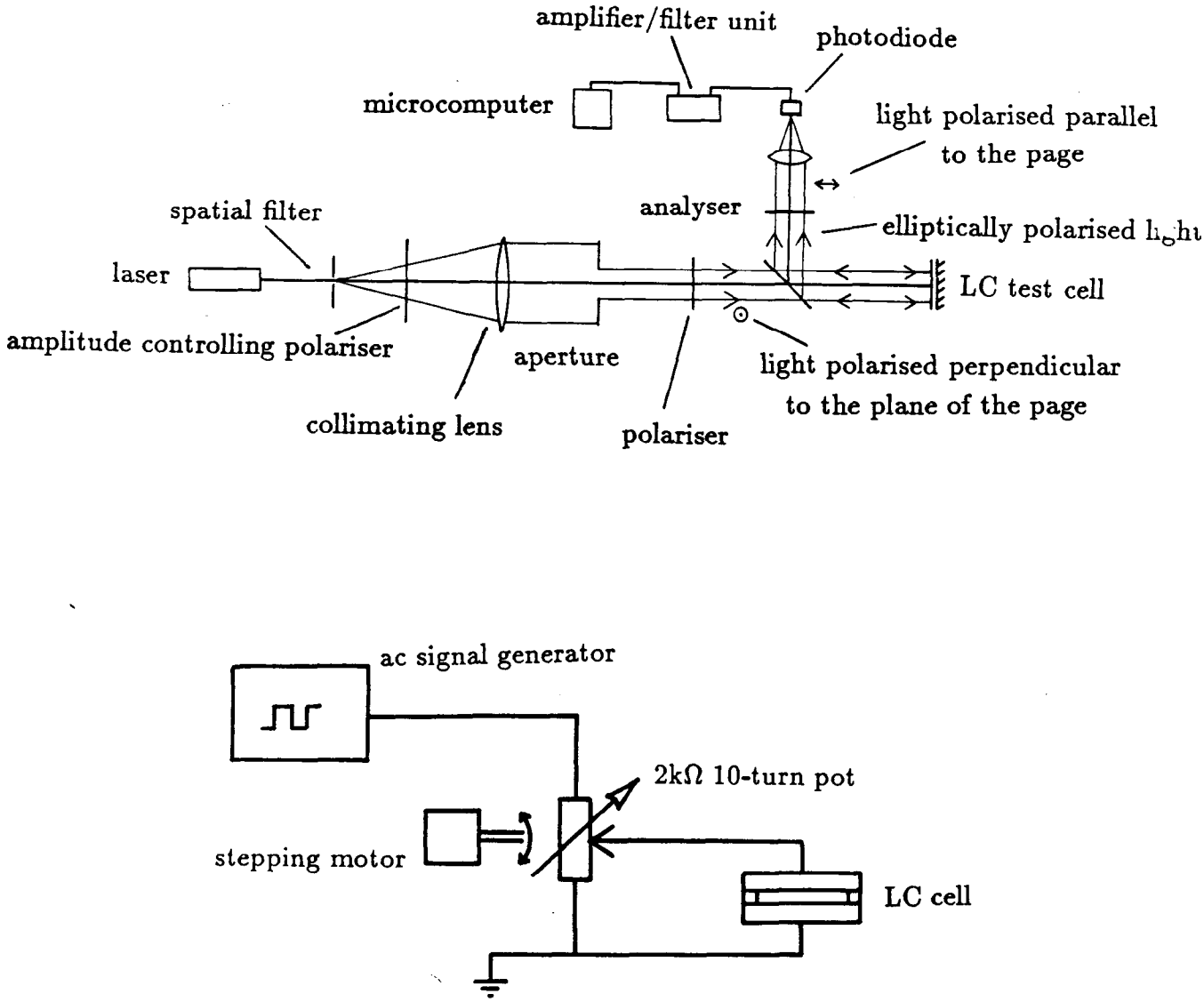

Figure 2.6: The liquid crystal cell test bench with (bottom) the LC drive scheme. The 10-turn potentiometer was controlled by a stepping motor which in turn was controlled by the microcomputer.

- A mirror was used in place of the cell to establish the true crossed position of the polaroids before the cell was inserted in the apparatus.
- The beam intensity and amplifier gain were set to exploit most of the dynamic range of the detector and the BBC ADC.

2. The time required to take the 480 measurements in each data set was about ten minutes and it was found that the laser power output varied by as much as 30% over this period of time. An analogue dividing circuit was designed to compensate for this variation but was later rejected in favour of a new, more stable, laser where output remained constant to better than 5%. Noise at this level was not considered to be important in the context of these measurements.

2.2.2 The test cells

Two types of reflection mode LC test cell were constructed. The first type was similar to the "standard" test cell shown in figure 2.2 and the second type was used as a test for some techniques useful in the construction of liquid crystal over integrated circuit SLMs. A photograph of the two types of cell is shown in figure 2.7. These cells differ in several respects, the most important of which is the thickness of the LC layer, and so they are sometimes referred to by this parameter.

The cell on the left uses two sheets of 3mm thick float glass supplied (by the Technical Glass Co.) with a transparent conductive coating of ITO on one side. Aluminium strips were evaporated[2] along one end of the glass sheets to enable good electrical connections to be made to the ITO. An aluminium mirror/electrode was deposited on the conducting surface of one of the pieces of glass. A rubbed PVA (Poly Vinyl Alcohol) alignment layer was used in this test cell. The slides were cleaned ultrasonically, dipped in a solution (1g in 400ml

[2]Aluminium and magnesium fluoride coatings were deposited by Andrew Garrie in the Special Techniques laboratory in the Physics department.

distilled water) of PVA and then allowed to dry for 24 hours in a laminar flow cabinet. All the handling of the glass after cleaning was done (wearing gloves) in a laminar flow cabinet in an effort to maintain cleanliness. The dry PVA was rubbed unidirectionally by sliding the glass plates four times, a distance of about 10cm, across a pad of clean lens tissue. Light finger pressure was used and a steel guide rule kept the glass moving in a straight line. The direction of rubbing was noted. Spacers were cut from a sheet of nominally 12μm $\pm$0.5μm thick polyester to determine the thickness of the LC layer in the cell, see figure 2.2. The cell was assembled using crocodile clips, over the spacers, to clamp the glass. Fairly firm pressure was used to help any settling of the spacer and two small blobs of epoxy adhesive were used to aid mechanical stability. The glass sheets were oriented at 45° to each other because it was found to be easier to rub the glass parallel to an edge than to use a template or jig to rub at 45°. The sense of the alignment was such that the rubbing directions were more nearly anti-parallel than parallel. This orientation was chosen because rubbed polymer alignment produces some pre-tilt, and this configuration minimises the splay deformation in the twisted nematic mono-crystal. The cell was filled with liquid crystal by capillary action. The British Drug House (BDH) mixture E7 was used. No heating was required to align the liquid crystal.

Rubbed PVA alignment was considered unsuitable for a LC cell built directly on an integrated circuit. It was decided not to rub the surface of the IC as the surface structures would be prone to damage. Also the pixel mirrors of the proposed SLM were anticipated to be about 45μm$\times$45μm in size and it was not clear whether the rubbing technique would produce good alignment over small, isolated, flat areas of a comparable size to the fibres of the rubbing cloth. An alternative alignment layer is obliquely evaporated magnesium fluoride which has the advantage that it does not involve mechanical contact with the IC. It should be possible to keep the surfaces clean and it may be a more repeatable technique than rubbing. Another technique which was considered to offer an improvement for SLM assembly was to substitute the polyester spacer with a photo-lithographically defined polymer spacer, this could be deposited during

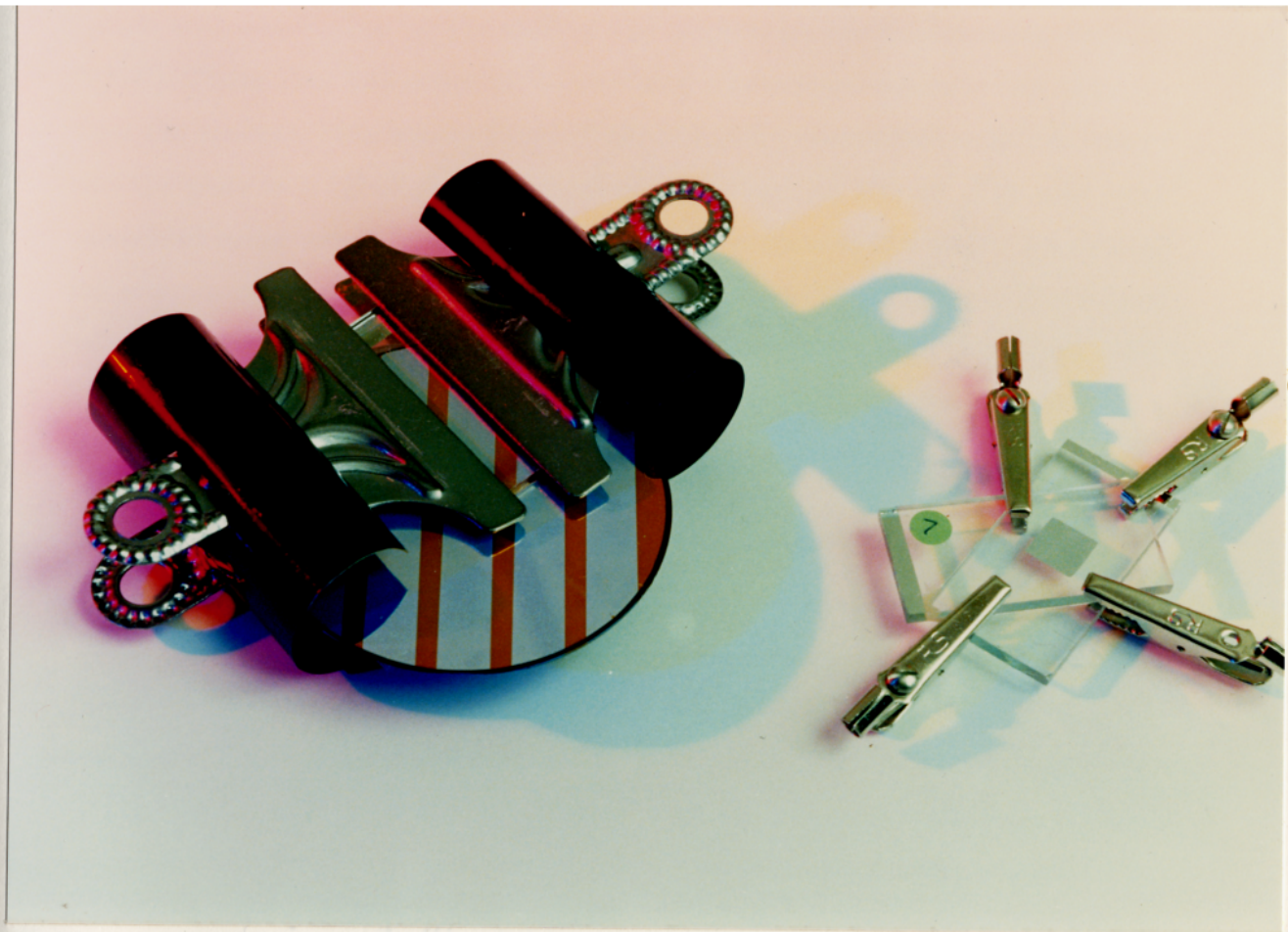

Figure 2.7: A photograph of the test cells. Both are 45° hybrid field effect cells filled with E7. The cell on the left was constructed on a blank integrated circuit wafer.

the chip fabrication process, exploiting the clean-room environment and the alignment facilities available in the wafer fabrication plant.

The second type of test cell incorporated these changes. Some blank wafers were coated with aluminium by the staff of the Edinburgh Microfabrication Facility (EMF). These then had strips of 3.7μm thick photo-resist deposited on them to form the spacers. Magnesium fluoride was obliquely evaporated onto the wafers and the glass to a thickness of approximately 150nm to 200nm. The cells were assembled using large "bulldog" clips to clamp the glass to the wafer. An optical flat was placed behind the wafer to give it some mechanical support. The 3.7μm cells were even more prone to particulate contamination than the 12μm cells. This sometimes caused short circuits by establishing current paths between the electrodes. The cells were filled, as before, by capillary action.

Test cell reflectance results

The test cells were illuminated normally with helium-neon laser light on the test bench (figure 2.6) and the measured reflected intensities are plotted in figures 2.8 and 2.9. The results are plotted with the peak reflectance normalised to unity. To estimate the absolute reflectivity an aluminium surface mirror (assumed reflectivity 90% [27]), was substituted for the test cells and a calibration measurement made. The polarisers were retained in order to allow for their absorption, but the analyser was rotated through 90°. The absolute peak reflectivities were 35% for the 12μm cell and 25% for the 3.7μm cell respectively. The contrast ratios — defined here as I_{max}:I_{0V} — were measured as $> 1000 : 1$ and $\approx 250 : 1$ for the thick and thin cells respectively. The form of the results is similar to those presented by Grinberg et al. [28]. It should be noted that very high contrast ratios can be obtained by optimising the spacer thickness for the particular wavelength of interest [44].

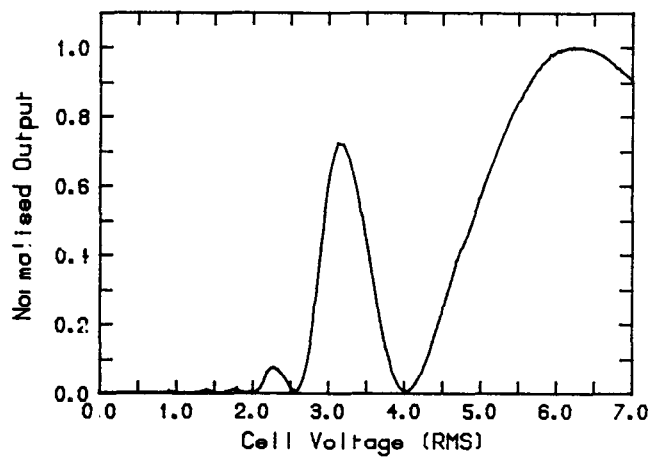

Figure 2.8: The reflectance of the 12μm thick hybrid-field effect test cell. I_{max}, the intensity measured at the maximum reflectance, was 35% of the input intensity. I_{max} occurred when the drive voltage was 6.23V_{RMS}.

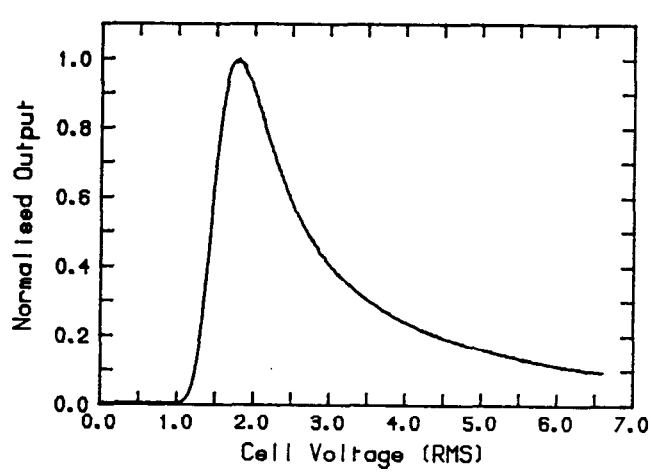

Figure 2.9: The reflectance of the 3.7μm thick hybrid-field effect test cell. The peak reflectance corresponds to a drive voltage of 1.82V_{RMS}.

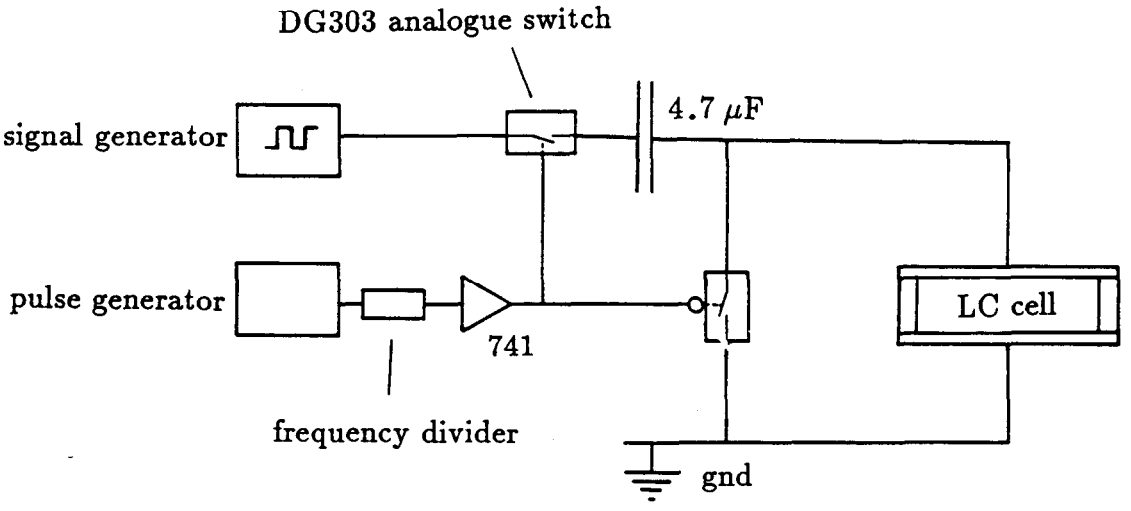

Figure 2.10: The liquid crystal test cell drive circuit used in the switching speed experiments. The analogue switch allowed the LC drive signal to be gated at any frequency down to about 1Hz. The complementary switch to ground closed when the switch to the signal generator opened; ensuring that there was no residual charge left on the cell which may have affected the switch-off times.

Switching speed

The switching speeds of the cells were investigated with a modified drive circuit, a schematic of which is shown in figure 2.10. The optical outputs of the cells were monitored with the detector and amplifier used in the reflectance measurements described earlier. The response speed of the measuring apparatus was not a limitation in any of the measurements. The electrical output was viewed on a storage oscilloscope. Switching times were measured for different on-state voltages. The most relevant times are those for the high transmission state voltages and these are tabulated below for switch "on" and switch "off".

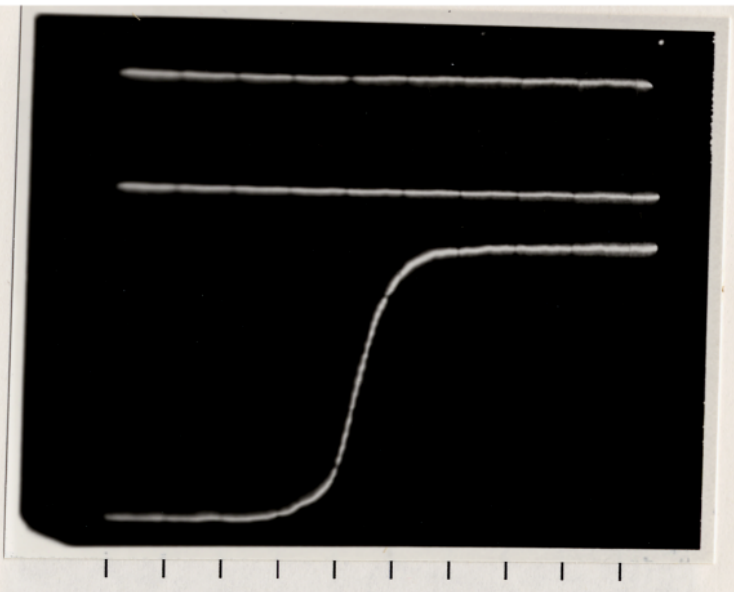

Figure 2.11: A 12μm HFE cell switching "on". The horizontal scale is 20ms/division. The top trace is the driving waveform — a square wave that is not resolved by the oscilloscope.

Cell	$0 \rightarrow 90\%$	$10\% \rightarrow 90\%$	$100\% \rightarrow 10\%$	$90\% \rightarrow 10\%$
12μm, 6.23V_{RMS}	100ms	30ms	150ms	$\approx$ 150ms
3.7μm, 1.82V_{RMS}	35ms	23ms	6.5ms	5ms

Photographs of the oscilloscope trace showing the cells switching are presented in figures 2.11 to 2.14. Certain aspects of these results are interesting. The switching speed of the thin cell is much greater than that of the thick cell. The switching time of twisted nematic structures is known to be proportional to the square of the layer thickness [8] and so, in the absence of other factors, thin cells are to be preferred. The delay before the onset of the optical response is significant compared to the switching time, especially for the thick cell. This effect is probably associated with the fact that significant deformations of the nematic structure can occur before polarisation guiding breaks down [8]. One consequence of this is that the delay between electrical stimulation and optical response depends on the time since the last excitation. This effect in the 3.7μm cell is illustrated in figures 2.15 to 2.17. These suggest that the liquid crystal does

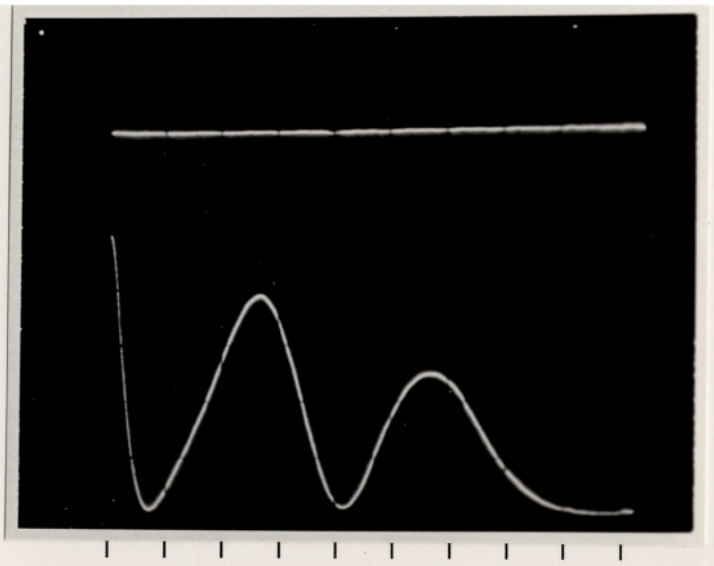

Figure 2.12: A 12μm HFE cell switching "off". The scale is 20ms/division.

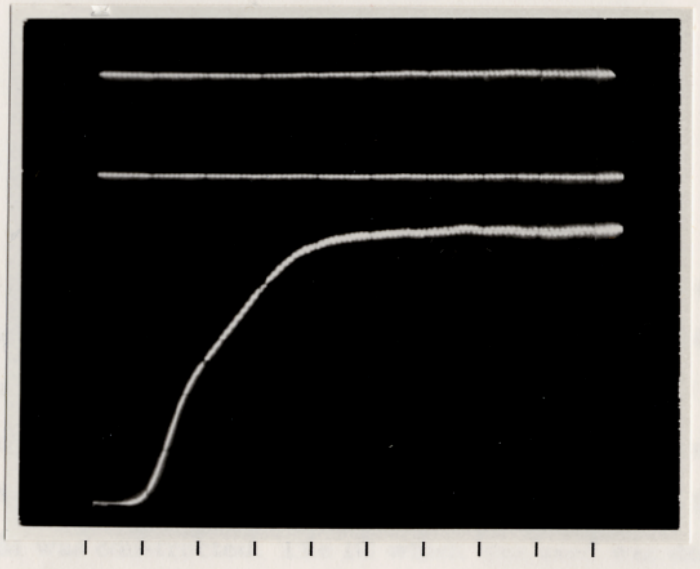

Figure 2.13: A 3.7μm HFE cell switching "on". The scale is 10ms/division.

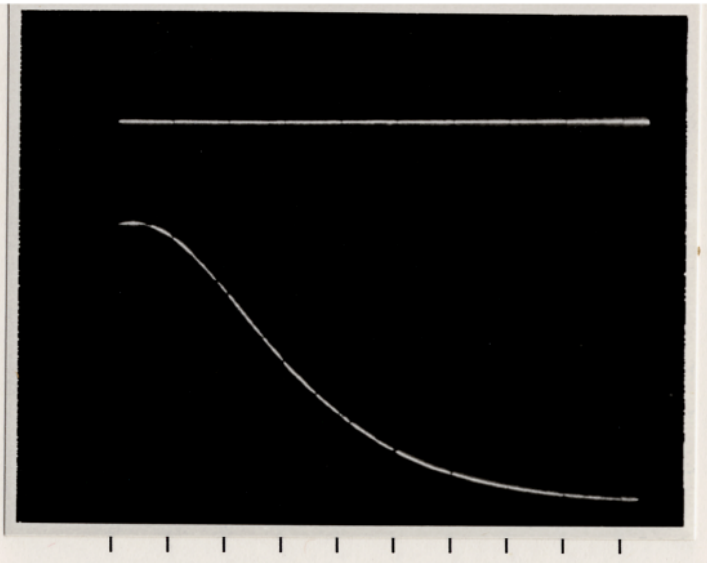

Figure 2.14: A 3.7μm HFE cell switching "off". The scale is 1ms/division. (Note the different scale from the switch-"on".)

not fully relax until about 100 milliseconds after the last switch-off, although the optical switch-off is much faster. The switch-off time is the same for all frame rates.

2.2.3 The 16 × 16 test SLM

At this stage it had been established that the hybrid field effect could be used in an amplitude modulating SLM with the expectation of acceptable contrast and switching speed. Thin cells are faster but it was not clear if the proposed integrated circuit technology would operate at a low enough voltage. To evaluate further the techniques of assembling a LC cell directly on an integrated circuit a prototype SLM was constructed. The IC which was used was designed by Ian Underwood [61] and had initially been used with a guest-host LC configuration, see section 1.2.2. An IC and a small (5mm by 5mm by 6mm thick) glass "cube" were prepared in the same way as the substrates for the thin test cells. The

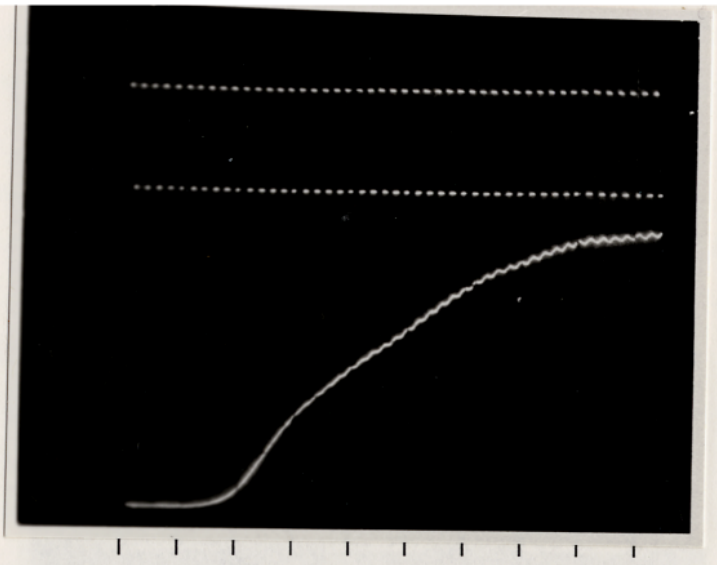

Figure 2.15: The switch-on response of a 3.7μm HFE cell after a 100ms delay since the last switch-off. A longer delay than this does not affect the switch-on time.

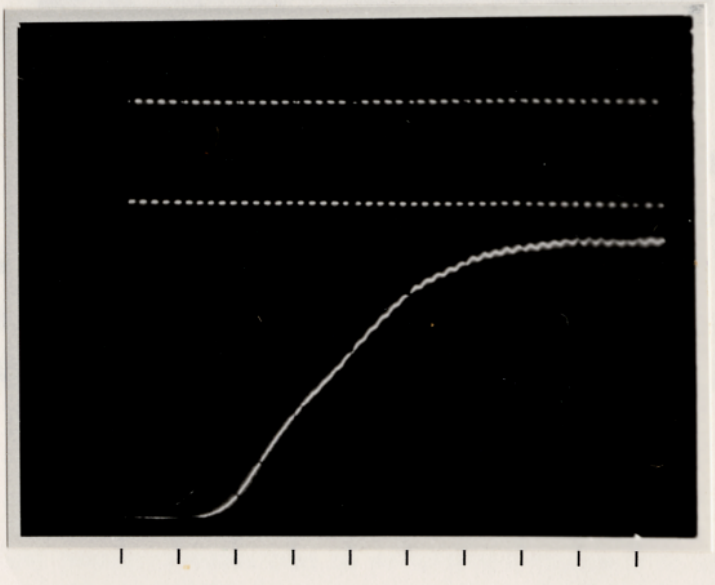

Figure 2.16: The switch-on response of a 3.7μm HFE cell after a 50ms delay since the last switch-off. The cell switches more quickly than in the previous case.

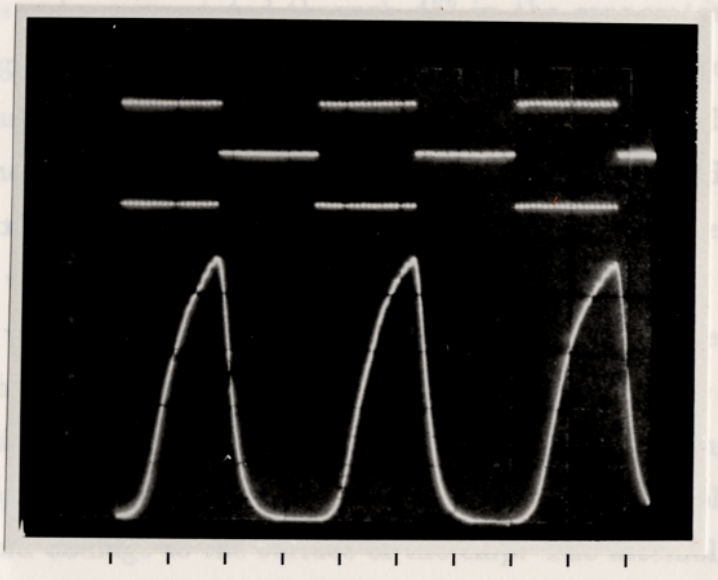

Figure 2.17: The "frame rate" was increased to the fastest rate which still allowed the output to reach 90% of the maximum. The time scale is 10ms/division and so this picture can be compared directly with figure 2.13 to see the effect that recent switching has on the switch-on time. The framing rate shown here is 28.5Hz. This is approximately twice as fast as would be expected from the earlier rise time measurements.

glass cube had two optically flat and parallel faces one of which was coated with ITO. Aluminium was evaporated onto the cube in such a way that it extended nearly all the way up one side, and also encroached onto the edge of the ITO coated surface. The aluminium provided an electrical contact to the ITO once the cube was assembled onto the face of the integrated circuit. The IC was packaged and bonded in the usual way. The magnesium fluoride alignment layer was deposited on the chip and the glass cube in the same way as on the test cells. The glass cube was rotated through 45° in the evaporator so that the required LC alignment occurred when the glass edges were parallel to the chip edges. A "U" shaped spacer was cut from 12μm polyester sheet. The spacer was positioned on the surface of the chip avoiding the array surface and the bonding wires. A perspex guide plate was glued to the top of the chip carrier with epoxy adhesive. Care was taken to establish a good glue joint round all four sides of the chip-carrier well, as the stability of the thickness of the LC layer depends on the rigidity of this component. A drop of liquid crystal (BDH, E7) was dropped on the centre of the array and the glass block was lowered through the guide plate onto the spacer. Care was taken to avoid trapping air bubbles in the LC layer and to avoid damage to the surface of the chip. The assembly was lightly clamped overnight to give time for excess LC to exude from the cell and for the spacer to settle. Epoxy adhesive was then used to hold the glass firmly in place. A wire was fixed to the aluminium on the side of the glass, and to a spare leg on the chip carrier, with some conductive paint. This wire allowed the transparent electrode to be electrically controlled through the usual type of IC holder. The method of assembly is similar to that used by Underwood [61] and is illustrated in figure 2.18.

The best 16 × 16 SLM was placed in an optical bench and imaged in coherent light. The optical bench is described in section 5.1 where it is used (in its full capacity) as a Fourier processing bench. Figure 2.19 is a photograph of the SLM displaying a test pattern. The top row of the chip was not addressable, because the chip was unfortunately incorrectly bonded to the chip carrier. The contrast appeared quite good when viewed by eye. A quantitative measure-

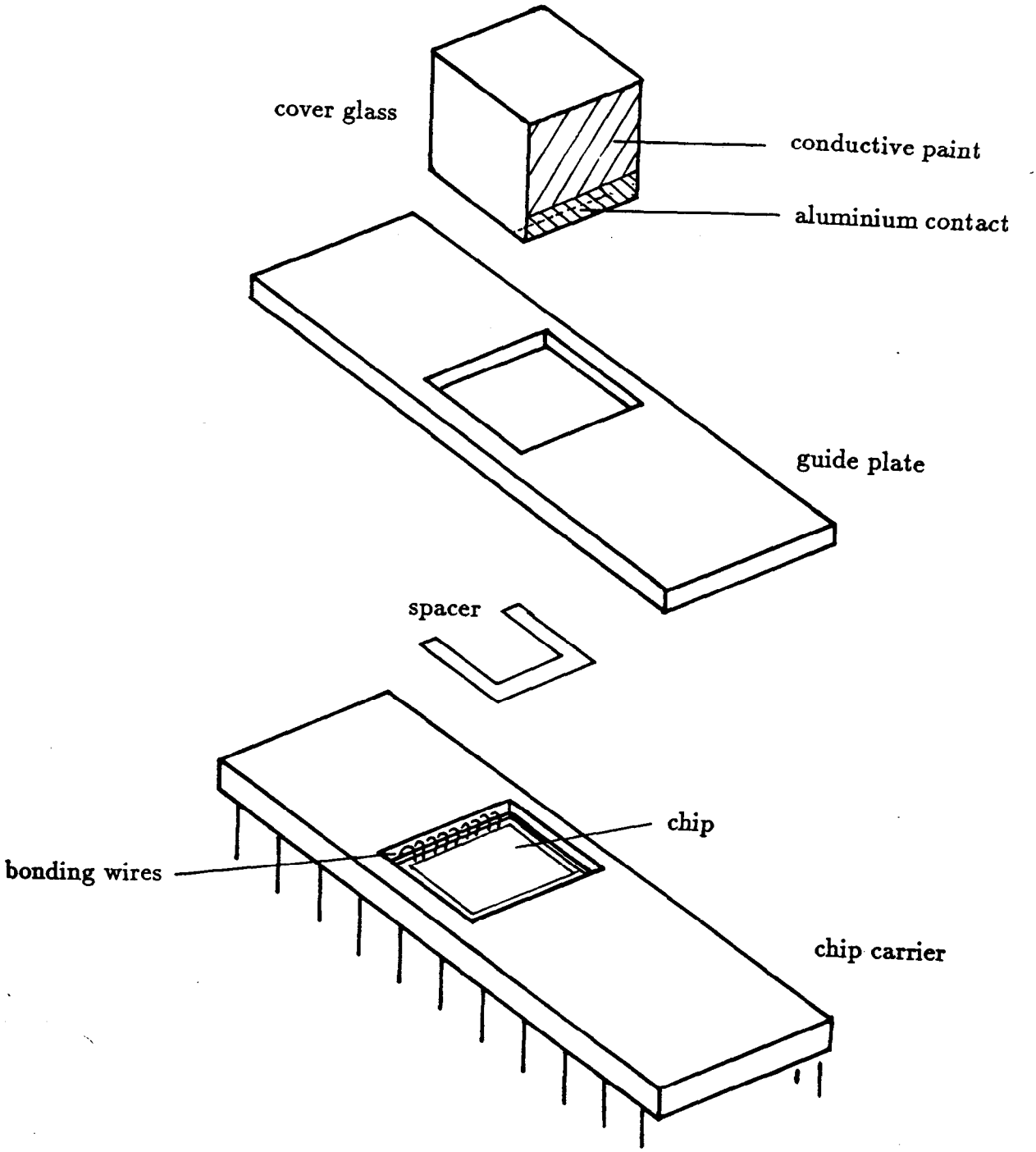

Figure 2.18: An exploded view of the the SLM assembly.

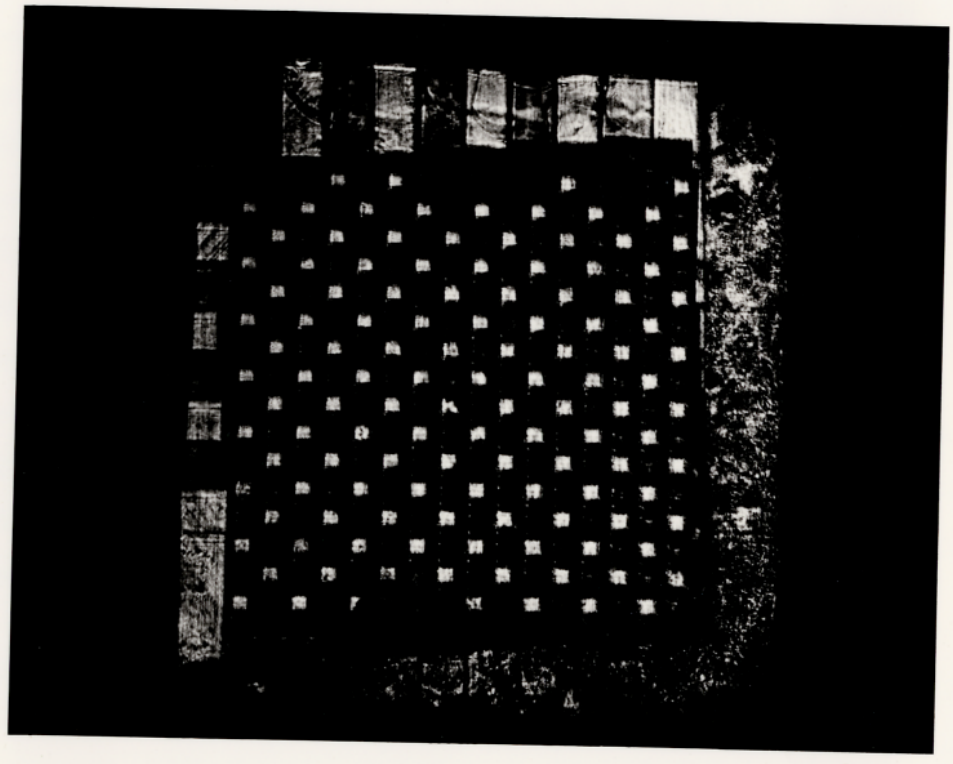

Figure 2.19: A test pattern displayed on the 16×16 SLM.

ment of the contrast ratio was made by imaging a single pixel onto a small ($250\mu m \times 250\mu m$) aperture fixed to the front of a photodiode (as used in the LC test cell experiments). Only the "active" part of the pixel was measured here — the pixel mirror. The small amount of light coming from partially activated LC over the surrounding circuitry was ignored. The contrast ratio, I_{ON}/I_{OFF}, was consistently 60–70 for most pixels. Individual pixel readings were found to be independent of the state of the rest of the array. The switching speeds were measured and found to be $\approx$ 100ms for both the switch-on and the switch-off operations (from initiation to 90% or to 10% respectively). These results are significantly different from those obtained from the test cells. The reduced contrast could be due to poor alignment or possibly some effect caused by slight heating of the LC by the IC. The 16×16 chip dissipates less than 60mW at 6V and so is not expected to warm by more than a few degrees. The pixels were examined in coherent light under a microscope and regions of poor extinction were seen. These regions appeared to extinguish at slightly different angles of polarisation, suggesting poor alignment of the LC layer. Two photographs showing regions of poor alignment are presented in figure 2.20. The slightly faster switching times could be caused by slight heating reducing the viscosity of the LC.

The objective of establishing that the hybrid field effect could be used for a liquid crystal over silicon spatial light modulator has been reached. The results for amplitude modulation, while not as good as might be expected from the test cells, were significantly better than any previous results from SLMs built on this type of chip [62] [50].

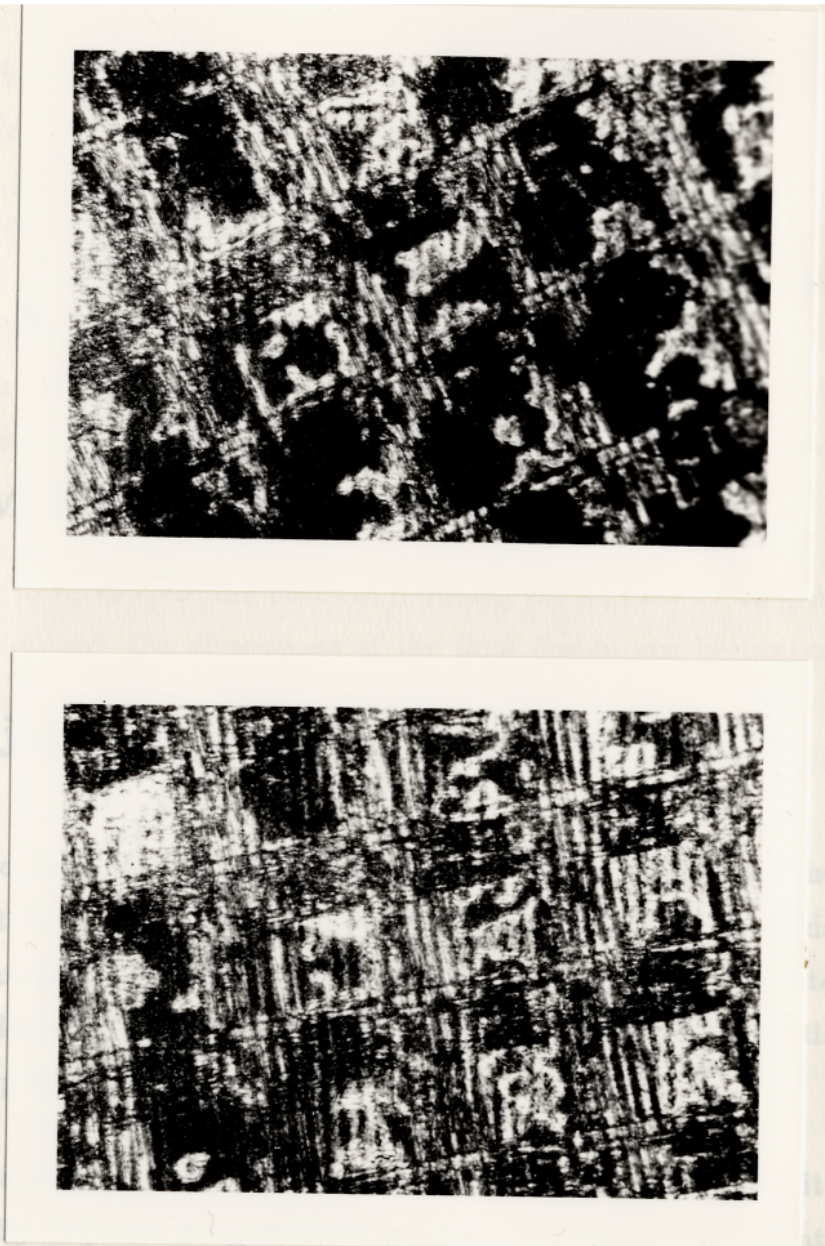

Figure 2.20: These two photographs, of an SLM, were taken through a microscope while the SLM was illuminated with polarised laser light. The readout is taken through a crossed analyser. The fringing is caused by the beamsplitter in the microscope. The SLM was rotated, on a stage, until the best extinction was found. The area shown had a generally poor extinction, and some of the pixels had regions which extinguished at a slightly different angle from the rest of the device. The bottom photograph shows the same area with the SLM rotated through 16° in an attempt to illustrate this. One of the pixels which most clearly shows this effect is the nearest (complete) pixel to the top right corner in the top photograph.